42 Trends in Glycolipid Biomarker Discovery in Neurodegenerative Disorders by Mass Spectrometry

Liana Dehelean, Mirela Sarbu, Alina Petrut, and Alina D. Zamfir

Abstract

Considering the devastating effects of neurodegenerative disorders and the increasing number of people affected by them, an early diagnosis even presymptomatic, prior to serious mental deterioration is necessary. Therefore, screening for biomarkers, especially glycolipids, in the biological matrices, either tissues or body fluids has proven to be of a great help in establishing an early diagnosis of the disease.

The present chapter, divided into three parts, highlights the implementation and modern applications of the most avant-garde mass spectrometry (MS) techniques characterized by speed, sensitivity and data accuracy for de novo identification and monitoring of glycolipids with potential biomarker role. The first section reviews the etiology, epidemiology, clinical picture, as well as the current diagnostic methods for four of the most frequent neurodegenerative disorders: Parkinson's disease, Alzheimer's disease, Lewy body dementia and frontotemporal dementia. The second section is dedicated to the role of glycolipids as biomarkers of these severe conditions. In the last part of the chapter, the state of the art in terms of mass spectrometry techniques for the detection of extremely valuable glycolipid biomarkers is described in detail. The proficiency of the MS, to be considered as and further developed into a routine method for early detection of neurodegenerative disorders, is also emphasized in the chapter.

Keywords

Neurodegenerative disorders · Dementia · Mass spectrometry · Glycolipid biomarkers · Gangliosides

42.1 General Considerations on Neurodegenerative Diseases

Dementia is an organic syndrome defined by global, acquired, progressive and spontaneously irreversible deterioration of the mind which affects predominantly cognition without impairment of consciousness. At least two or more cognitive functions are impaired, such as memory, attention, reasoning, or perception. Non cognitive symptoms are also present, such as anxiety, depression, emotional control impairment or disturbed social behavior.

Dementia is the consequence of either brain injuries (strokes, tumors, infections, traumas) or systemic conditions with impact on brain function (metabolic, endocrine, vitamin imbalances, heavy metal, carbon monoxide or alcohol/recreational drug poisoning). The individual's ability to care for him/herself or to perform everyday activities is impaired requiring assistance mainly in the moderate and severe phases.

Dementia, also referred as chronic organic syndrome, should be differentiated from delirium (confusional state), which is an acute and potentially reversible organic syndrome defined by clouding of consciousness. In addition,

Liana Dehelean and Mirela Sarbu contributed equally to this work.

L. Dehelean (✉)
University of Medicine and Pharmacy "Victor Babes", Timisoara, Romania
e-mail: lianadeh@umft.ro

M. Sarbu · A. Petrut
National Institute for Research and Development in Electrochemistry and Condensed Matter, Timisoara, Romania

A. D. Zamfir
National Institute for Research and Development in Electrochemistry and Condensed Matter, Timisoara, Romania

"Aurel Vlaicu" University of Arad, Arad, Romania

A. G. Woods, C. C. Darie (eds.), *Advancements of Mass Spectrometry in Biomedical Research*, Advances in Experimental Medicine and Biology 1140, https://doi.org/10.1007/978-3-030-15950-4_42

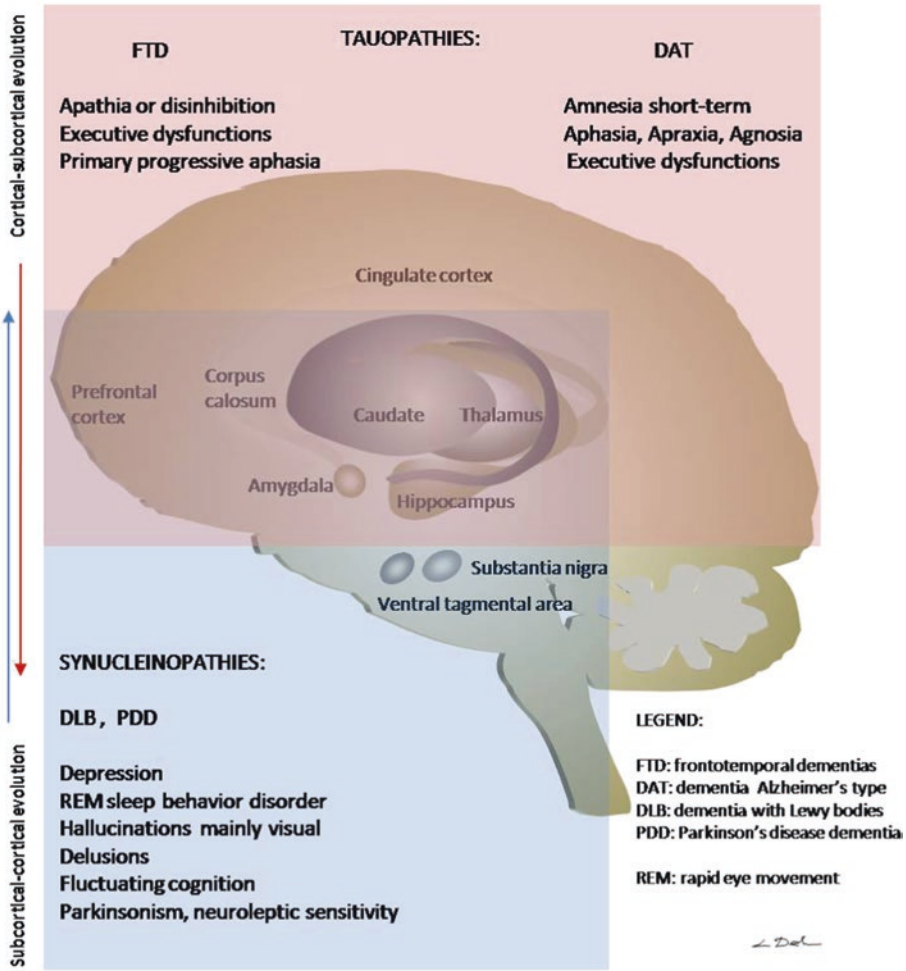

Fig. 42.1 Clinical and anatomical features of tauopathies and synucleinopathies

dementia has to be distinguished from amnestic syndromes confined to memory loss, or depression in elderly (pseudodementia).

In the DSM-5 dementias are called major neurocognitive disorders by contrast to minor neurocognitive disorders formerly referred as mild cognitive impairment.

The genetic, clinical and pathogenic overlaps between different types of dementias generated debates whether some of the dementias are distinctive pathological entities on a continuum (Fig. 42.1). Fronto-temporal dementias and dementia of Alzheimer's type are classified on pathological grounds as tauopathies (as the result of abnormal accumulation of tau protein), while dementia in Parkinson's disease and Lewy body dementia are classified within the synucleinopathies (as a consequence of synuclein protein abnormal accumulation). There is evidence that tau protein and alpha-synuclein influence each other explaining the clinical and pathologic overlaps between tauopathies and synucleinopathies [1, 2].

42.2 Neurodegenerative Diseases: Etiology, Epidemiology, Clinical Picture and Diagnosis

42.2.1 Dementia in Alzheimer's Disease (Dementia of Alzheimer's Type, DAT)

DAT is the most frequent dementia accounting for about 50% of all dementias. It is more common in women and after the age of 65.

The causes are unknown (primary degenerative dementia), but the most important risk factors are age, female gender, family history and personal history of head injury. Early-onset familial DAT is the consequence of dominant autosomal mutations involving genes on chromosomes 21 (gene for amyloid precursor protein, APP), chromosome 14 (gene for presenilin 1), and chromosome 1 (gene for presenilin 2). As the genes for APP, presenilin 1 and 2 account for about one-half of early-onset familial DAT, other unknown

genes may be involved in the etiology of DAT. Late-onset, sporadic DAT is associated with the presence of ε-4 allele of the apolipoprotein E (ApoE) gene on chromosome 19 coding for an apolipoprotein with a low affinity for β-amyloid. Homozygous carriers of this allele are at risk of developing early-onset DAT.

Macroscopic changes show atrophy of the cerebral hemispheres mainly involving medial temporal lobe and the hippocampus. The volume loss has a posterior-anterior gradient. Structural imaging evidences atrophy of temporal and parietal lobes (computer tomography, CT and magnetic resonance imaging, MRI). In the late stages diffuse cortical atrophy is reflected by ventricular, sulcal and pericerebral space enlargement. Functional neuroimaging shows bilateral temporo-parietal hypoperfusion (single photon emission computed tomography, SPECT) and bilateral temporo-parietal hypometabolism evidenced by the reduction in oxygen and glucose metabolism measured as decreased FDG uptake (fluorodeoxyglucose—positron emission tomography, FDG-PET). The microscopic changes are the diagnostic markers of DAT and are represented by: extracellular β-amyloid plaques, intracellular neurofibrillary tangles (phosphorylated tau protein), and granulovacuolar degeneration of hippocampal neurons. Amyloid plaques and neurofibrillary tangles are also present in normal aging subjects, but the high number and the pattern of distribution (entorhinal cortex, hippocampus, amygdala, neocortex and basal nucleus of Meynert) are characteristic for DAT. Beta-amyloid is a peptide involved in lipid homeostasis, decreasing the level of cholesterol in the lipid rafts [3]. These are microdomains of the membrane that are rich in cholesterol and sphingolipids being involved in synaptic transmission. In turn, cholesterol enhances the activity of gamma secretase (containing presenilin 1 and 2) which will produce β-amyloid. Abnormal amounts of β-amyloid (due either to the overproduction through anomalous APP cleavage or to the impaired clearing by low affinity ApoE4) will polymerize and become insoluble forming the amyloid plaques. There are complex interactions between ApoE4 and β-amyloid, and there is data suggesting that ApoE4 may be involved in DAT in a way that is independent of β-amyloid [4, 5]. The tau protein is involved in stabilizing the neuronal microtubules. These have a structural role as being part of the neuronal cytoskeleton and a functional one providing the axonal transport of proteins and organelles synthesized by the nucleus. Hyperphosphorylation of tau protein results in depolymerization of microtubules and formation of neurofibrillary tangles in the place of former neurons. Therefore, the density of neurofibrillary tangles correlates with the severity of cognitive deficits. Because the enzyme glycogen synthase kinase-3β (GSK-3β) is considered to be involved in hyperphosphorylation of tau protein and its activity is stimulated by β-amyloid, there is a possibility that β-amyloid may trigger the cascade of changes seen in DAT. There is also evidence of other interactions between β-amyloid pathway and neurofibrillary tangles formation [6].

Regarding neurotransmission, a selective loss of cholinergic neurons appears mainly in the nucleus basalis of Meynert. This nucleus is the main source of acetylcholine in the brain and its neurons project diffusely into cortex and hippocampus being involved in cognition. Both the loss of choline acetyltransferase (involved in acetylcholine synthesis) and of nicotinic receptors (on which acetylcholine binds) may further contribute to the cognitive impairments. Another neurotransmitter involved in memory consolidation is glutamate. It is the main excitatory neurotransmitter of the brain. It is considered that dead neurons release glutamate, which through excessive stimulation induces neurodegeneration of the remaining ones (glutamate neurotoxicity).

The first structure to be affected by degeneration is the hippocampus, which is part of the Papez circuit involved in short-term memory. As a result, patients with DAT will present short-term memory impairment (forgetfulness for recent events and difficulty of learning new information), while long-term memory loss appears in final stages. Memory impairment often leads to a secondary delusion of prejudice. As the degeneration progresses to more posterior temporal and parietal lobes, word finding difficulties (anomia), semantic and sensorial dysphasia/aphasia, dyspraxia/apraxia, dysgnosia/agnosia, dysgraphia/agraphia, dyscalculia/acalculia appear. Occipital lobes degeneration accounts for visuospatial impairments reflected by difficulties in appreciating distances and orientation in space, prosopagnosia and alexia. Frontal lobes degeneration is responsible for reduced and stereotyped thought content, impairment in working memory leading to difficulties in performing mental operations simultaneously, abstract reasoning problems, executive dysfunctions (organizing, planning, monitoring, and consequence anticipation), release of primitive reflexes and incontinence. Executive dysfunctions impair judgment and problem solving making independent living difficult and the patient dependent on entourage. Mood changes (anxiety, depression, irritability) associated with behavioral disturbances (restlessness, wandering, hoarding), and sleep-wake inversion are common. The insight for the cognitive decline is absent and patients often find excuses for their functional impairment. Later in the evolution, seizures and mild extrapyramidal signs appear.

The definitive diagnostic is based on histopathology (biopsy or necropsy). A diagnosis of possible or probable DAT is supported by noninvasive brain imaging and clinical examination. Brain or systemic diseases impairing cerebral function should be absent. Current research focuses on cerebrospinal fluid (CSF) biomarkers such as tau, phosphorylated tau, and β-amyloid (Aβ) 1–42, which may differentiate DAT from normal aging and other forms of dementia.

The onset of DAT is insidious and the progression is slow. In most cases, the survival rate from diagnosis to death is about 8 years. The cognitive decline rate is of about 3 points/year measured with mini mental state examination (MMSE). In early-onset familial cases the survival rate decreases at 4 years.

Treatment consists in pharmacological and non-pharmacological approaches. Medication addresses the cognitive decline and behavioral issues. Cholinesterase inhibitors (restoring the cholinergic deficit) in association with a glutamate NMDA receptor antagonist (to prevent glutamate excitotoxicity) are indicated in moderate to severe cases [7]. Emotional and behavioral disturbances are addressed with sedative–hypnotic, antipsychotic, antidepressant and mood stabilizing medication. The non-pharmacological approaches are represented by behavioral therapy techniques (suppressing unwanted behaviors and reinforcing the desired ones), reality orientation, validation therapy, art, music and activity therapy (providing meaningful stimulation to improve self-esteem, socialization, well-being, and exercise), bright-light therapy (to improve fluctuations in diurnal rhythms), and multisensory approaches [8]. Correcting age related sensory deficits is also important.

In clinical practice, the dementia syndrome appears years after the first β-amyloid plaques are deposited in the brain or Alzheimer's disease-like CSF Aβ1–42 positivity appears [9]. As medication is more effective in the early stages, it is critical for the later evolution to diagnose and treat dementia as soon as possible. Current CSF biomarkers (low Aβ42, elevated total tau and phosphorylated tau) are identified and measured using invasive lumbar puncture. Low CSF Aβ42 appears in asymptomatic subjects. CSF total tau is a marker of neurodegeneration indicating the current intensity of neuronal injury. It is assumed that mild cognitive impairment is correlated with neurodegeneration. The noninvasive imaging biomarkers showing abnormal radioactive tracer retention, such as amyloid PET [10] and tau PET [11] are considered expensive. Other minimal or noninvasive biomarkers for Alzheimer's disease (AD), such as circulatory micro ribonucleic acid (miRNAs) biomarkers, blood based amyloid markers, inflammatory markers and oxidative stress markers are under research [12].

Recently, the National Institute on Aging and Alzheimer's Association (NIA-AA) issued a research framework updating the 2011 guidelines for AD with the purpose to create a system for diagnosing and staging AD on a continuum based on the new developments in biomarkers' research [13]. It is not conceived for clinical practice, but to unify the research methodology. The AD continuum includes preclinical and clinical AD. Preclinical AD refers to a stage characterized by lack of overt symptoms in opposition to clinical AD represented by mild cognitive impairment (MCI) and DAT (with its mild, moderate and severe stages). New biomarkers were added, such as cortical amyloid PET ligand binding (imaging the amyloid plaques in cortex and blood vessels), CSF Aβ42, CSF Aβ42/Aβ40 ratio, and cortical tau PET ligand binding imaging for neurofibrillary tangles. A scheme—AT(N)—was conceived using both CSF and imaging biomarkers: (1) A refers to aggregated amyloid beta or associated pathologic state and is evidenced by low CSF Aβ42, low Aβ42/Aβ40 ratio and Amyloid PET; (2) T refers aggregated tau (neurofibrillary tangles) or associated pathologic state and is evidenced by elevated CSF phosphorylated tau (P-tau) and Tau PET; (3) (N) refers to neurodegeneration or neuronal injury and is evidenced by MRI, FDG-PET, CSF T-tau (CSF total tau).

Using the AT(N) profile it is possible to diagnose and stage subjects at risk of developing or having DAT. In this respect, a person with a A+T-(N)- biomarker profile is referred as having Alzheimer's pathological change. In the case of the A+T+(N)- or A+T+(N)+ profile, the person has AD, where N offers information about the staging of the disease. Profiles such as A-T+(N)-, A-T+(N)+, A-T-(N)+ are classified under non-AD pathologic change. In summary, A+ puts the subject in the Alzheimer's continuum. A+T+ are both required for AD, while the non-specific N biomarker is used to describe the severity of the changes. The N biomarker also indicates a comorbid non-Alzheimer's pathologic change as in the A+T−N+ profile. A separate cognitive staging (C) was added. Cognitively unimpaired subjects with A+T-(N)- are referred as preclinical Alzheimer's pathologic change. Subjects with A+T+(N)- or A+T+(N)+ profiles who are cognitively unimpaired are referred as having preclinical AD, while those with mild cognitive impairment are referred as AD with MCI or prodromal AD. When dementia is clinically diagnosed, then the patients with A+T+(N)- or A+T+(N)+ profiles are referred as having AD with dementia (DAT).

42.2.2 Cortical Lewy Body Disease or Dementia with Lewy Bodies

Dementia with Lewy bodies (DLB) represents up to 10–15% of all dementias and 20% of late-onset dementias. Risk factors are old age (more common after 60 years old) and male gender.

The etiology of DLB is unknown (primary degenerative dementia). DLB shares clinical and pathologic features of both Alzheimer' and Parkinson's diseases. In 50% cases of DLB, pathologic findings reveal generalized brain atrophy with amyloid plaques and neurofibrillary tangles as in DAT. By contrast to DAT there are less neurofibrillary tangles. There is also pallor of substantia nigra, free neuromelanin, neuronal loss and gliosis as in Parkinson's disease dementia (PDD), although these changes are less pronounced.

By contrast to PDD, in DLB, Lewy bodies are widespread in brainstem, limbic system and cerebral cortex. DLB is more sporadic (frequent ε 4 allele) than familial. A gene on chromosome 2 and duplications or triplications of the gene for alpha-synuclein are genetic risk factors for DLB.

The main macroscopic change in DLB is the depigmentation of substantia nigra, while microscopic features include: neuronal loss with Lewy bodies and Lewy neuritis (dystrophic neuronal processes) in the surviving neurons, free neuromelanin, and gliosis. All these changes are less severe in comparison with PD. Lewy bodies (LB) are eosinophilic intracellular cytoplasmatic inclusions composed mainly of α-synuclein (which aggregates forming insoluble fibrils) and ubiquitin. Alpha-synuclein is a protein involved in synaptic vesicle synthesis. Ubiquitin is a regulatory protein involved in protein degradation using the proteasome. In this respect, LBD is classified as a synucleinopathy as PD. By contrast to PD, in LBD, LB are present in midbrain (substantia nigra, locus coeruleus, dorsal raphe nucleus), but more widespread in the limbic system (hippocampus, amygdala), in the nucleus basalis of Meynert, cingulate and insular cortices, as well as in frontal and temporal lobes. There is a correlation between the density of the LB in the nucleus basalis of Meynert and the severity of the cognitive impairment. Another correlation was found between the presence of visual hallucinations and the density of LB in amygdala, parahippocampus, and inferior temporal lobes. While amyloid plaques are found in the cerebral cortex, the neurofibrillary tangles are as frequent as in normal subjects. Structural neuroimaging (CT and MRI) shows generalized cortical atrophy which is more severe in the parietal and occipital lobes. By contrast to DAT, there is less temporal or hippocampal atrophy. Functional neuroimaging reveals low dopamine transporter uptake in basal ganglia (PET) and medial parietal and occipital hypoperfusion (SPECT).

Both dopaminergic and cholinergic neurotransmission are impaired in DLB. The activity of acetylcholine in the cerebral cortex is low and the loss of choline acetyltransferase and acetylcholinesterase are more severe than in DAT. There is a correlation between the loss of cortical choline acetyltransferase activity and the severity of cognitive impairment. The dopamine in the basal ganglia (caudate nucleus) is reduced.

The clinical picture of DLB includes symptoms and signs found both in DAT and PDD making the differential diagnosis difficult. The onset of cognitive symptoms should be simultaneously or within a year of the motor (parkinsonian) symptoms, otherwise PDD should be considered. Verbal memory is less impaired than in DAT. Visuospatial function is severely affected. The patient has no insight for the cognitive decline. The extrapyramidal syndrome (Parkinsonism) is spontaneous though bradykinesia and limb rigidity are more common than tremor. There is a pronounced propensity to develop Parkinsonism when conventional antipsychotics are prescribed. The level of consciousness is fluctuating. Patients experience transient and recurrent falls and loss of consciousness due to carotid sinus hypersensitivity. Complex visual hallucinations appear in clear consciousness. Hallucinations in non-visual modalities, as well as systematized delusions of persecution unrelated with the memory impairment build up a schizophrenia-like syndrome. Non cognitive symptoms, such as depression and enacted dreams (vivid dreams with vocalizations and complex motor behavior during rapid eye movement (REM) sleep referred as REM behavior disorder) are common.

Diagnosis is based on clinical findings, while there are no laboratory specific tests for DLB. Polysomnography may show the loss of normal atonia during REM sleep. Brain or systemic diseases impairing cerebral function should be absent.

The onset is insidious and progression is gradual. The rate of cognitive decline is double or three times more rapid than in DAT, while the progression rate of Parkinsonism is similar to PD. The survival time after diagnosis is of 8 years.

As in DAT, for cognitive symptoms cholinesterase inhibitors are prescribed. Hallucinations and delusions are treated with antipsychotics. Conventional antipsychotics (neuroleptics) should be avoided because they can worsen Parkinsonism through dopamine D2 antagonism or may produce neuroleptic malignant syndrome. The parkinsonian syndrome is addressed with dopaminergic therapy, which in turn may worsen the existing hallucinations and delusions.

42.2.3 Fronto-temporal Dementias (FTD)

The fronto-temporal dementias are represented by a group of neurodegenerative diseases where the atrophy is restricted to the frontal and temporal lobes. Among these, the classic Pick's disease is included.

FTD represent the majority of presenile dementias, and about 5–10% of all dementias (the third most common degenerative dementias after DAT and DLB).

The cause of neurodegeneration is unknown (primary degenerative dementia). In 40–50% of cases the etiology is genetic, with an autosomal dominant transmission. Several chromosomes are involved: chromosome 17 (gene for microtubule associated protein tau, MAPT, gene for progranulin associated with Parkinsonism), chromosome 9 (gene for valosin containing protein, VCP, associated with comorbidity of dementia with inclusion body myopathy and Paget's Disease of the bone, or the C9ORF72/chromosome 9 open reading frame 72 mutation associated with comorbidity between FTD and amyotrophic lateral sclerosis, ALS), and chromosome 3 associated with familial ALS.

Three forms of FTD are described: Pick's disease with neurons containing Pick bodies and ballooned Pick cells, frontal lobe degeneration with neuron loss and gliosis without Pick bodies and ballooned Pick cells (spongiosis in the frontal lobe) and dementia with motor neuron disease which associates frontal lobe degeneration and amyotrophic lateral sclerosis.

The macroscopic changes are represented by the atrophy of the frontal lobes (mainly posterior inferior areas) and of the anterior part of the temporal lobes. The main microscopic features include: neuronal loss of cortical pyramidal cells, enlarged, vacuolar and chromatophilic neurons called Pick neurons (in Pick's disease), frontal neurons and glial cells with Pick bodies. These are argentophilic inclusions of hyperphosphorylated tau protein, transactive response DNA-binding protein 43, TDP-43, and ubiquitin. In those forms associated with motor neuron disease, the inclusions are ubiquitin positive and tau negative. The loss of neurons is seen as a cortical vacuolation (spongiform degeneration) and is replaced by astrocytic gliosis. There is also myelin loss.

Although fronto-temporal dementias and DAT are considered tauopathies, by contrast to DAT, the density of neurofibrillary tangles and senile plaques are normal for age. Based on the nature of the protein inclusions FTD are now classified in three subtypes: fronto-temporal lobar degeneration with MAPT (tau positive inclusions), fronto-temporal lobar degeneration with TDP-43 (tau negative, ubiquitin positive inclusions) and fronto-temporal lobar degeneration with fused in sarcoma, FUS protein [14] represented by tau negative, ubiquitin positive but TDP-43 negative inclusions).

Structural neuroimaging reveals fronto-temporal atrophy (CT or MRI). Functional neuroimaging shows fronto-temporal hypoperfusion (SPECT) and hypometabolism (PET).

Regarding the neurotransmission, there is evidence for postsynaptic cholinergic deficit with presynaptic and postsynaptic serotoninergic deficits.

The clinical forms of fronto-temporal dementia depend on which brain areas are predominantly affected and are represented by the behavioral FTD (bvFTD) and the language form of FTD. The behavioral FTD form is characterized by a frontal lobe syndrome. Both frontal lobes are affected. Depending on the specific localization of the atrophy, two different clinical manifestations are possible. When the dorsolateral frontal cortex is impaired, symptoms such as apathy (emotional blunting), decreased motivation, mutism, social withdrawal and neglect of personal hygiene, appear. By contrast, when the orbito-medial frontal cortex is impaired, disinhibition dominates the clinical picture accompanied by impulsive behavior, restlessness, distractibility, overactivity, bulimia with preference for sweets, hypersexuality or inappropriate sexual behavior, breaching of etiquette, loss of empathy, repetitive and compulsive behaviors (echolalia, perseverative and stereotyped speech and movements). Other signs of frontal lobe dysfunctions are the deficits of the executive function (planning, organization, self-monitoring, and consequences prediction) affecting judgment and decision making, release of primitive reflexes, and urinary incontinence. The insight is lost.

The language form of FTD is called primary progressive aphasia (PPA) and has also two clinical manifestations depending on the impaired areas. The frontal predominant form known as progressive nonfluent (expressive, motor, anterior) aphasia (PNFA) is manifested by a gradual loss of speech fluency, speech simplification, word-finding difficulties, circumlocutions, phonemic paraphasias, effortful and telegraphic speech, and early mutism, while comprehension is intact. In this case, the posterior and inferior parts of the frontal lobe are affected. Semantic aphasia or progressive fluent (anterior) aphasia is dominating the clinical picture when the inferior part of the temporo-parietal cortices is affected. It is manifested by semantic anomia (loss of isolated word meaning), impaired isolated word comprehension with preserved phrase comprehension, effortless fluent speech which is grammatically correct but nonsensical. It is accompanied by visual agnosia, dysgraphia, and dyslexia. Repetition is preserved. Temporal lobe impairment is also manifested by stereotyped behavior (counting, hand-clapping, hoarding useless things). In summary, the early signs of FTD involve severe behavioral (personality) or speech changes, whereas memory, praxia and spatial orientation are preserved. Calculation is also maintained until the middle stage of the disease. Some patients may develop Parkinsonism secondary to mutations on chromosome 17.

The onset is insidious between 50 and 60 years with slow or rapid progression. The survival rate from diagnosis to death is about 8–9 years as average, and 3–5 years in subjects with associated motor neuron disease.

There is no specific treatment. Behavioral disturbances are treated with antipsychotics, antidepressants (selective serotonin reuptake inhibitors) and sedatives. Emotional changes are treated with mood stabilizers. Treatment with acetylcholinesterase inhibitors and memantine has shown limited efficacy.

42.2.4 Parkinson's Disease Dementia (PDD)

Parkinson's disease dementia is a type of degenerative dementia caused by Parkinson's disease (PD). Dementia develops late in the evolution of PD, after 10 years on average [15]. Conventionally, the one year rule applies: PDD is diagnosed

when dementia appears at least 12 months after the onset of Parkinsonism, otherwise DLB is considered.

PDD occurs in 2% of subjects over 65 years. 20–40% of patients with PD will develop dementia in the late stages of the disease.

In PDD, dementia is secondary to PD. The latter is mainly idiopathic (the sporadic forms of PD). Familial forms of PD have an earlier onset and are autosomal dominant involving genes on chromosome 4 (Park 1 gene coding for α-synuclein) and chromosome 12 (Park 8 gene coding for LRRK2/Leucine-rich repeat kinase 2—dardarin), or autosomal recessive concerning genes on chromosome 6 (Park 2 intervening in ubiquitin–proteasome system) and chromosome 1 (Park 6/PINK 1/PTEN induced putative kinase, and Park 7/DJ-1). Mutations in the LRRK2 are associated with the accumulation of synuclein, tau, neither, or both proteins [16] explaining the shared pathologic and clinical findings between dementias.

The macroscopic changes in PD refer to depigmentation of substantia nigra, of ventral tegmental area and of locus coeruleus which appear pale. Microscopic changes include: melanin containing neuronal loss with Lewy bodies intracytoplasmic inclusions and Lewy neurites present in the remaining neurons (less than 20% of initial number) gliosis, and increased free neuromelanin. The ubiquitin–proteasome processes the degradation of α-synuclein. Abnormal folding of α-synuclein results in its aggregation into fibrils forming the Lewy bodies in the perikaryon and Lewy neuritis in neuronal dendrites and nerve terminals. These are toxic for the dopaminergic neurons in substantia nigra and ventral tegmental area. The spread of the Lewy bodies progresses from brain stem (dorsal vagal nucleus, locus coeruleus, substantia nigra, ventral tegmental area, raphe nuclei) and the olfactory bulbs towards limbic system (hippocampus, amygdala, cingulate cortex) and cerebral cortex. When Lewy bodies reach the cerebral cortex and the basal nucleus of Meynert, PDD appears. Structural neuroimaging (CT and MRI) shows increased distance between the two caudate nuclei with ventricular enlargement, while functional neuroimaging (SPECT and PET) shows bifrontal and biparietal hypometabolism in patients with PDD.

The degeneration of the midbrain substantia nigra affects the nigrostriatal dopaminergic pathway. Loss of dopaminergic neurons in the midbrain substantia nigra results in an imbalance between dopamine and acetylcholine. Unopposed by dopamine, acetylcholine will induce the Parkinsonian motor symptoms (rigidity, akinesia and resting tremor). Degeneration of the midbrain ventral tegmental area affects the mesocortical and mesolimbic dopaminergic pathways. The deficit of dopamine in the mesocortical circuit impairs the prefrontal cortex function with executive dysfunctions while in the mesolimbic pathway it is correlated with the risk of depression and psychosis. Norepinephrine and acetylcholine dysfunctions result in autonomic dysregulations (orthostatic hypotension, urogenital impairments and constipation) and are possibly correlated with the presence of LB in locus coeruleus, dorsal vagal nucleus, sympathetic ganglia and myenteric and submucosal plexus in the digestive tract [17]. Cholinergic dysfunction in laterodorsal and pedunculopontine nuclei involved in wakefulness and REM sleep is responsible of REM sleep behavioral disorder. The presence of REM behavioral disorder in PD may signal cholinergic denervation in neocortical, limbic and thalamic circuits [18]. Norepinephrine and serotonin dysfunctions are also involved in the mood changes accompanying PD. Dopaminergic denervation characterizes the early stages of PD, while progressive cholinergic denervation is associated with dementia.

Parkinsonian motor symptoms must precede dementia. The pathognomonic triad refers to rigidity, akinesia and unilateral resting tremor. Dementia appears later in the evolution with impairments in the working memory and retrieval of explicit memory. By contrast to the DLB, the visuospatial function is intact in early stages. Other deficits involve hyposmia, orthostatic hypotension, urinary incontinence and urgency, erectile and ejaculatory dysfunctions, constipation and seborrheic dermatitis. Psychiatric symptoms are common, such as depression (in about 40% of subjects and in all stages of the disease), anxiety and psychosis (in later stages) with visual hallucinations and paranoid delusions. REM sleep behavior disorder usually precedes Parkinsonism in 80% cases with 4 years. The pattern of LB spread from lower brain stem and olfactory system to higher brainstem and neocortical areas explains why olfactory dysfunction and REM sleep behavior may antedate the classical Parkinsonian triad.

PD is characterized generally by an insidious onset and slow progression. Depression, hyposmia or REM sleep behavior may be preclinical markers of PD [19], while dementia appears in later stages of the disease.

The motor symptoms of PDD are treated with dopaminergic therapy (carbidopa-levodopa) with a very good response in the early stages. Side effects consist in psychotic symptoms, dyskinesias, on-off phenomenon, and impulsive–compulsive behaviors. Anticholinergic drugs are more effective in treating tremor and rigidity, but have side effects such as cognitive deficit, confusion, hallucinations, dry mouth, constipation and urinary retention. Adjunctive treatments refer to amantadine, pramipexole (dopaminergic agonist), and selegiline (MAO/monoamine oxidase B inhibitor). Cholinesterase inhibitor drugs, antidepressants, anxiolytics and antipsychotic drugs address associated dementia, depression, anxiety or psychosis.

42.3 Glycolipids as Brain Biomarker

The development of the brain, one of the most complex organs, is a protracted process involving specific well-defined stages of growth and maturation. A pivotal role in this lifelong process is played by the cellular membrane, a thin semi permeable membrane layer. Represented as a lipid bilayer (Fig. 42.2), with lipids and proteins as principal components, and carbohydrate groups, in a lesser extent, attached to some of the lipids and proteins, forming glycolipids and glycoproteins, the cellular membrane acts as a barrier between the inner and outer environment by allowing certain ions and organic molecules into the cell while keeping others out.

Among these, the glycolipids, due to their amphiphilic character determined by the hydrophilic sugar headgroup and the hydrophobic lipid tail responsible for anchoring the molecule in the membrane, exhibit distinctive physicochemical properties and bioactivities.

Situated outside of the cellular membrane into the aqueous phase, the carbohydrate moiety of the glycolipids is acting as ligand, improving the cohesion and structure of the membrane and facilitating the interaction with molecules dissolved in the surrounding environment. With a variable composition from small saccharide units up to large polysaccharide chains, the sugar core, not just influence some membrane parameters, like fluidity and domain formation (lipid rafts) [20], but also determine a diversity of biological functions essential for various processes in life. Therefore, glycolipids are key players with distinctive biochemical roles in cell–cell interactions, recognition activities, cellular proliferation, transformation, adhesion, aggregation and differentiation, as well as in immune response and the blood type [21, 22]. Moreover, glycolipids are responsible for the function adjustment of several membrane-associated proteins, giving rise to valuable intra- and extracellular mediators [23].

In order to preserve the functional integrity of the nervous system, the sphingolipids, an important class of glycolipids participate in the nervous system to numerous signalling pathways to control the neuronal survival, migration and differentiation, reaction to trophic factors, synaptic stability and transmission, as well as the formation and stability of central and peripheral myelin [23].

Crucial for the glycolipid structural variability and their functionality are on one side the expression and intracellular distribution of glycosyltransferases, responsible for assembling one by one the proper sugar moiety to a certain lipid molecule, so that the correct receptor can be activated on the cell which responds to the presence of the glycolipid on the

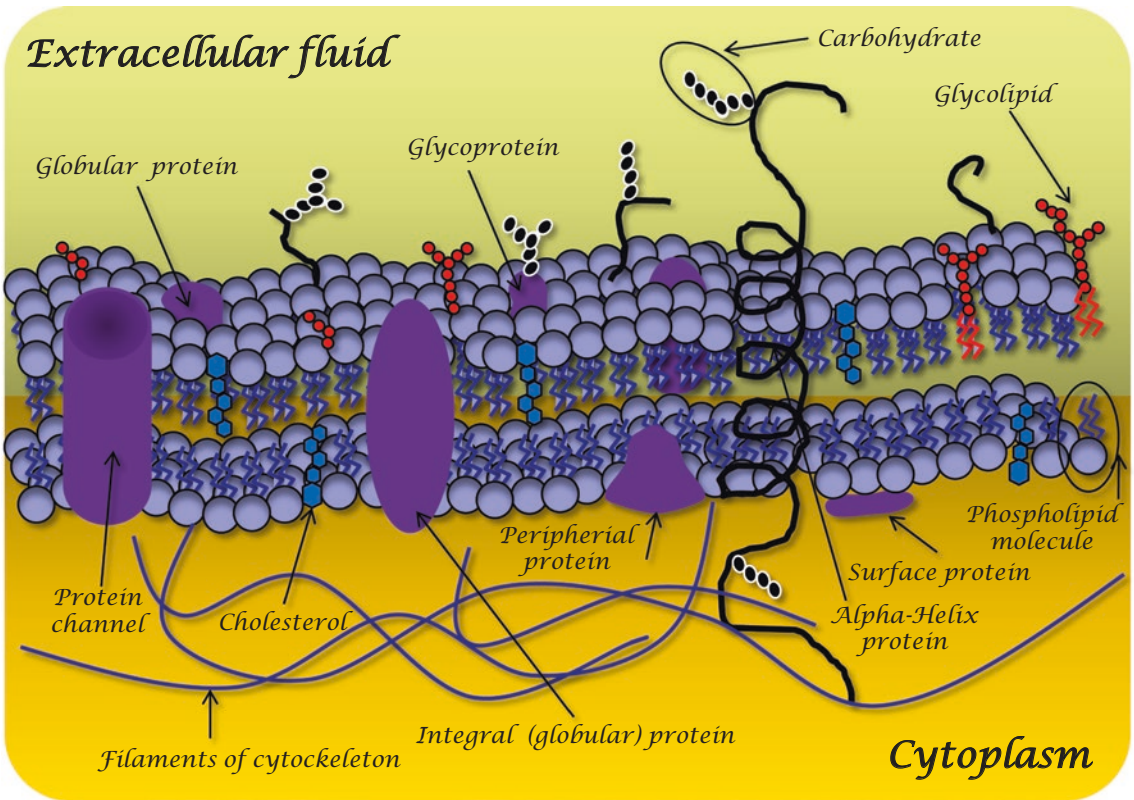

Fig. 42.2 The structure of the plasma membrane represented as a fluid mosaic diagram with the hydrophilic heads pointed outward and the hydrophobic tails oriented towards the inner side of the bilayer

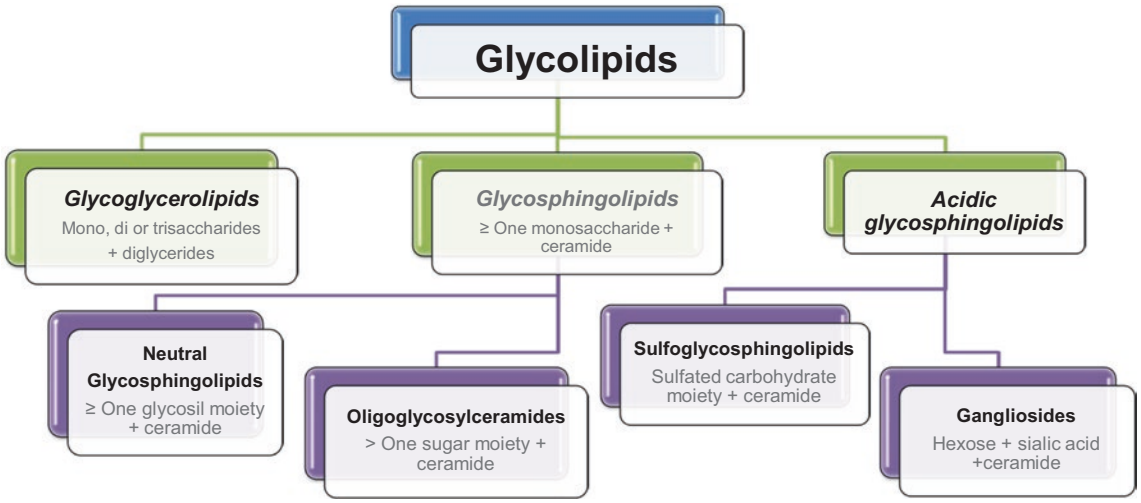

Fig. 42.3 The main glycolipid classes based on the nature of sugar and lipid moieties

surface of the cell [24], and on the other side, of glycoside hydrolases, responsible for glycosidic bond cleavages leading to modified oligosaccharide structure or back to unmodified lipids. The simplest glycolipids are perhaps the cerebrosides, in which a singular sugar unit, glucose (Glc) or galactose (Gal) is linked to a ceramide (Cer). Mostly located in nervous tissue where are responsible for cell signaling and intercellular communication, [25], glycosphingolipids (GSLs) are generated by the attachment of more than one sugar residue to the ceramide core (Fig. 42.3). The glucosylceramide (GlcCer) serves as the source of most GSLs, including the complex glycolipids, such as gangliosides (GGs), that are found to contain elaborated and branched oligosaccharide cores made of Gal, Glc, *N*-acetylgalactosamine (GalNAc) and sialic acid (*i.e.* *N*-acetylneuraminic acid, Neu5Ac) [26].

The GGs represent about 10–20% of the lipids content in the neuronal membrane [27]. The major GG species of the brain are GM1, GM2, GM3, GD1b, GT1b, GQ1b, GD1b/a. Of these, GM1 representing 15% of the total GGs of the myelin in peripheral nerves [27, 28], is of particular importance since it exerts neurotrophic or neuroprotective effects under a variety of circumstances, influencing various cellular activities at the level of plasma and intracellular membranes, among which Ca^{2+} homeostasis, mitochondrial function, and lysosomal integrity [29–31].

In view of the over 300–400 GSL species identified [32], each of it with different sugar chain structure and different role in the normal physiology of the brain, any abnormal deviation on their synthesis or degradation pattern leads to various types of neurodegenerative disorders, mental diseases, stroke and central nervous system (CNS) traumas. The essential role of lipids and glycolipids in tissue physiology and cell signaling is revealed by the elevated number of neurological and neurodegenerative diseases caused by unregulated metabolism [23]. Several disorders, broadly known as lysosomal storage diseases, with huge impact on life quality and lifetime, due to CNS developmental delay, mild-to-severe mental retardation, seizures and profound neurodegeneration, leading finally to vegetative state, are known to be caused by mutations in gene encoding glycoside hydrolases. Consequently, cell dysfunction and clinical malformations are generated by a sphingolipid metabolism deeply deregulated, an altered membrane organization and abnormal sphingolipid patterns. Therefore, the accumulation and storage of glycolipids which can no longer be degraded by the enzymes [33], is responsible for the occurrence of gangliosidosis (Tay-Sachs and Sandhoff disease), Guillain-Barré syndrome, Krabbe, Gaucher, or Fabry disease.

Due to the immense combinatorial and structural diversity of the biological lipidomes encoding for varied cellular and membrane functions, large-scale characterization and quantification analysis are required in order to understand the relation between glycolipids and neurodegenerative disorders, the complex lipid-lipid and lipid-protein interactions and dynamics, and to distinguish between pathogenic and nonpathogenic glycolipids within samples containing different glycolipid isoforms [23].

The glycolipidomics has rapidly developed as an emerging field with a tremendous contribution to monitor delicate changes and detect specific biomarkers in diverse collection of glycolipids in cells and tissues. All of these are now possible due to the development of avant-garde molecular biology and laboratory technology, and to "-omics" revolution through the development of databases, informatics, bioinformatics and biostatistics [34]. The currently available hardware and software platforms, employing histological examination of the affected tissue, DNA analysis, expression arrays, immunological tests, enzyme activity measurement, nuclear magnetic resonance, electrochemical

and laser-induced fluorescence detection, separation techniques and mass spectrometry [34] are applied to detect and characterize molecular components.

The glycolipidomics research is focused on the identification and quantification of the thousands of cellular glycolipid species in order to map the whole population in a biological system and identify specific biomarkers for various physiological and pathological processes. Therefore, the structure, function and dynamics of cellular glycolipids, as well as the changes that arise during perturbation of the system, are in the focus of researchers.

Plasma membrane glycolipids provide the primary attachment sites for a wide range of infectious and amyloid proteins [35]. Probably one of the most important and devastating result of this metabolism deregulation is the anomalous sphingolipid-protein interactions, responsible for the misfolding procedures determining the fibrillogenic and amyloidogenic processing of disease-specific protein isoforms, such as Aβ peptide in AD and α-synuclein in PD [23].

Several studies have demonstrated the strongly affinity of the soluble form of Aβ to major brain ganglioside molecular species, especially to GM1, a monosialotetrahexosylganglioside, which is often found in lipid rafts [36–42], leading to the formation of GM1-ganglioside-bound Aβ (GAβ) complex. Upon this binding, Aβ adopts an altered conformation, being converted from random coil to an ordered structure rich in β-sheet [43]. Therefore, it was hypothesized that GAβ acts as an endogenous seed for the assembly of amyloid fibrils in the AD brain [39, 44–47].

According to the literature, an important pathological hallmark of aging and neurodegeneration processes, such as the ones associated with AD, are the membranes physicochemical properties alteration due to neural loss and brain shrinkage. Since GGs are enriched in neurons, their altered metabolism causes discrepancies in the lipid proportion in membranes and/or changes in ratios of lipid membrane [48–52]. Earlier studies have evidenced that the degree of GG alteration is directly influenced by the age of AD onset. While in early-onset or familial AD cases the GG concentration decreases up to 58–70% in gray matter and to 81% in frontal white matter as compared with the control brains, in late-onset cases, a significantly reduction in concentration was observed only in the temporal cortex, hippocampus, and frontal white matter [50]. Considering the important role of GM1 in the formation of Aβ plaques, its metabolism and the spatial information on the distribution of GM1 in the AD brain is of great interest. An increased concentration of ganglioside GM1 in the cortex [53], cerebrospinal fluid [54] and platelets [55] of AD, as well as a significantly higher amount of GM1 and GM2 in the frontal and temporal cerebral cortex of individuals with AD and frontotemporal dementia [56] as compared with controls, was reported. Therefore, these findings support the idea that this increased amounts of GM1 and GM2 in lipid rafts, might be connected with the formation of toxic amyloid fibrils [57] and can be used as biomarkers for AD discovery.

Changes in the pattern of other gangliosides in AD brain, not just of GM1 were also illustrated. Kracun et al. reported a considerable diminished content of the major brain ganglio-*N*-tetraosyl-series ganglioside species (GT1b, GD1b, GD1a, and GM1) in both the frontal and temporal cortex and basal telencephalon in the brain of patients with AD *vs*. the respective areas in control brains [51, 52]. Concurrent with a significant decrease of GT1b and GD1b, Brooksbank and McGovern [58] and Crino et al. [59] showed a slight increase in GT1a, GD3, GM1, and GM2, suggesting therefore the direct connection within an abnormal GG metabolism and the affected cortical areas of neurodegeneration that afflicts AD. Such variations are not just attributed to accelerated lysosomal degradation of GGs and/or reactive astrogliosis, but also to an increased catabolism activity of acidic β-D-galactosidase and a diminished activity of sialyltransferase, which are specific for neuronal death.

Hirano-Sakamaki W. et al. demonstrated that the spatial arrangement/ distribution of GM1 molecular species in the AD hippocampus could also serve as biomarker [60]. By comparing the GM1(d20:1/18:0) to GM1(d18:1/18:0) ratio in hilus, granule cell layer (GL), inner and outer molecular layer (ML), in order to evaluate the distribution of GM1(d18:1/18:0) and GM1(d20:1/18:0) and differences between control and AD, a decrease in the ratio of GM1(d20:1/C18:0) to GM1 d18:1/C18:0) in the outer ML of the dentate gyrus was observed. Because the region of main input into the hippocampus is represented by the outer ML, their results strongly suggest that such a decrease in C20/C18 ratio may play a causal role in AD or can be correlated with the progression of the disease [60].

If the neuronal development and regeneration are known to be ganglioside-related processes, the anti-ganglioside antibodies were found to exhibit a reverse activity. Therefore, their presence in various biological matrices, especially of anti-GM1 antibody, was used by several researchers as brain biomarkers and associated to neuronal degeneration in AD, multi-infarct dementia and PD with dementia [61–63]. However, in 2014, through an enzyme-linked immunosorbent assay, Miura Y. et al. [64] measured the serum levels of anti-ganglioside antibodies in patients with clinically diagnosed AD, and vascular dementia and compared them to sera of normal controls, patients with Guillain-Barré syndrome (GBS) and multifocal motor neuropathy (MMN), diseases where the antibodies are thought to be pathogenic. Following this study, they have demonstrated that titers of IgG and IgM anti-GM1, anti-GQ1bα, and anti-GT1aα antibodies did not differ among AD, vascular dementia, and normal controls, suggesting that the anti-GG antibodies are unlikely to be pathogenic in AD or useful as biomarkers [64].

With a pivotal role in cholinergic synaptic transmission and cognitive function [65], cholinergic-specific antigen-1α (Chol-1α) were reported also in sera of patients suffering from AD [66, 67]. Ariga T. et al. [68] reported an increase in content of Chol-1α antigens, GQ1bα and GT1aα, both with high affinities to Aβs, in the brain of transgenic mouse AD model. Although these GGs are normally minor species in the brain, they represent evidence for generation of cholinergic neurons in the AD brain, as a result of compensatory neurogenesis activated by the presence of Aβ and may be used as markers of cholinergic neurons [69].

With aging, an increase of GM1 expression in the human brain concomitant with a diminished GM3 content occurs [70], both species being involved in the pathophysiology of AD and PD [70–73]. The neurodegenerative process allied with Parkinson disease is as well dependent on the content in GG species since α-synuclein, an inflammatory stimulant for microglia, is a GM1-binding protein [74, 75], while GM2, GM3 and asialo-GM1 have a weaker bound on α-synuclein [76]. Through this bounding, the fibrillation of α-synuclein and its pathological accumulation is averted.

Up to now, several hypotheses for the aggregation of α-synuclein protein responsible for not just for PD, but also for DLB exist. One of the hypothesis ascribe the aggregation/accumulation of α-synuclein on the absence of both a and b series of GGs in brain [77, 78], especially of GM1 [79]. A diminished content on GM1 is caused by deletion of β-1,4-*N*-acetylgalactosaminyltransferase 1 (GalNac-T) liable for transferring GalNAc onto GM3 and GD3 gangliosides leading to GM2 and GD2, and so, the conversion into GM1 and GD1. Significant reduced expression of GM1, GD1a, GD1b and GT1b were reported in PD brain as compared with control brain [80, 81]. On the other side, higher levels of IgM antibodies against GM1, GD1b and GQ1b gangliosides in the sera of patients who suffered from idiopathic PD in comparison with healthy age-matched individuals were reported [76]. These results are a hallmark of the PD pathogenesis.

Additionally, causative mutations in the helical region of α-synuclein (34-KEGVLYVGSKTK-45), a specific motif identified to be conserved also in Aβ peptide (fragment 5–16) [82], disrupt its helicity and hampers the GM1 binding [74, 83, 84]. Perhaps the most important risk factor allied with sporadic PD, as described in the literature, is the incidence of mutations in the gene of the lysosomal enzyme glucocerebrosidase, GCase (GBA1) [85]. A diminished activity of GCase is translated into the accumulation of glucosylsphingosine and GlcCer/GluCer in the lysosome due to a reduced degree of conversion of this substrate to glucose and ceramide. Such accumulation not just compromises the lysosomal activity [86–89], but also damages the lysosomal recycling process, inducing an increase of defective lysosomes incapable for autophagic clearance of α-synuclein and therefore, an elevated level of the protein [87]. Consequently, the bidirectional effect of α-synuclein and GCase forms a positive feedback loop through which GlcCer can stabilize α-synuclein and prevent its degradation, and α-synuclein, in turn, inhibits GCase [86]. Consequently, consistent with previous reports implicating lower GCase activity in the CNS [90–92] and in the periphery, one of the most significant differences between PD and controls was reported in several occasions to be the higher concentration of GM3 [93–96], a PD biomarker candidate. Nevertheless, although in the ample study of Alcalay R. N. and collaborators, from the investigated lipid subclasses, GM3 concentration had the most significant difference between PD and controls (14.5%), suggesting its clear association with PD, they propose a combination of GM3 levels with other measurements for a diagnostic value [97].

Furthermore, the increased level of GlcCer and α-synuclein in brain, associated with an increased level of other sphingolipids such as lactosylceramide, GD3, GM2 and GM3 [86, 97], substantiate a clear relationship within the disruption of sphingolipid metabolism and the PD pathology. Moreover, α-synuclein was also demonstrated to interact with GM2 and to contribute to neurodegeneration *via* a comparable feedback loop [75, 79]. This occurs in Tay-Sachs and Sandhoff diseases, both of them associated with development of Lewy bodies and synuclein aggregates [98, 99], where the degradation of GM2 is inhibited due to a deficiency of hexosaminidase A and/or B. Additionally, the increased lyso-GM2 levels in the plasma and brain of patients with Sandhoff disease, as well as in the plasma of Tay-Sachs patient uphold the concept of lyso-GM2 as potential biomarker of Tay-Sachs disease and Sandhoff disease [100].

In 1980, for the first time, the parkinsonism was correlated with Gauche disease (GD) [101], an inherence driven as well by accumulation of GlcCer due to mutations (approximately 300 different mutation identified up to now) in the *GBA1* gene. Thus, patients with PD are five times more likely to carry *GBA1* mutations than healthy controls [102], while those with adult onset GD exhibit up to 20-fold higher chance of developing parkinsonism or diffuse Lewy body disease [103–105]. Besides this increased risk in developing PD, the Gaucher patients also present an elevated GM3 content, supporting therefore a possible link between GCase activity, elevated GM3 and PD [106]. Various studies conducted by comparison on the glucosylceramide, glucosylsphingosine and GM3 content in plasma from treated and untreated Gaucher disease patients were carried out. All of them confirmed that, compared to normal individuals, the concentration of GluCer in GD patients treated with enzyme replacement therapy is still increased (seven times higher), while in GD patients not receiving treatment is significantly higher (17 times higher) [93, 94, 107, 108]. Hence, besides the hallmark GM3, the quantification of GluCer accumulated

in GD represents a sturdy candidate as a biomarker for this pathology [109] and can be used in complementary diagnosis and as a means of monitoring the treatment [108].

Up to now, most of the studies conducted for the identification of biomarkers in neurodegenerative disorders involved the use of post-mortem tissue samples, since in most of the cases, a definite diagnosis required autopsy documentation of pathology. Nevertheless, the CSF and the blood glycolipid levels were also studied in some extent to distinguish if it can be used as an indicator or predictors of disease progression. A blood-based biomarker would be preferable because the blood draw could be accessed easily and inexpensively in a clinical setting especially when repeated measures are needed for tracking disease progression or therapeutic response. However, due to the blood–brain barrier, which limits the passage of various molecules into the blood, and complicates the correlation of peripheral markers and brain processes, the development of blood-based biomarkers for neurodegenerative diseases is rather complicated.

In view of the overwhelming effects of neurodegenerative disorders, their increased incidence, as well as the diversity and complexity of the involved biological glycolipids and their minute amount in tissues and body fluids, advanced analytical technologies specialized on characterization and quantification are therefore highly required. Hence, the following section of the paper highlights the broad applications of the most advanced mass spectrometry techniques, indispensable analytical tools characterized by high sensitivity, for a precise molecular level elucidation of the glycolipids involved in different neurodegenerative disorders and the discovery of specific biomarkers, that can further be used to track the evolution of the disease or the response to a treatment.

42.4 Discovery of Glycolipid Biomarkers by Advanced Mass Spectrometry

Glycolipids exhibit a high structural diversity in tissues and cells, which is determined by the complexity of their composition and their tissue- and cell-specificity. The discovery of glycolipid species that play a biomarker role for certain diseases and of species involved in or even responsible for some physiological or pathological processes requires the development of methods that allow for highly accurate comparative analyses of single species expressed in the diseased *vs.* normal tissue [110]. In recent years, high performance thin layer chromatography (HPTLC), immunochemical and immunohistochemical methods performed that service to some extent, by demonstrating the differences in the composition and amounts of glycolipids in various matrices as well as their distribution onto the cell surface [111]. The experimental results obtained by using the aforementioned techniques, were, however, only able to provide data on the major glycolipid components [110]. Moreover, HPTLC, the immunochemical and immunohistochemical methods, helpful for species identification, were found inadequate for their structural analysis, which is a major drawback in the case of research projects focused on biomarker discovery, since, in many instances, minor structural differences were shown to be highly useful in discriminating between a real biomarker and a ubiquitous compound.

These shortcomings of HPTLC and immunochemical methods are attributable to the reduced sensitivity achieved so far in glycolipidomics and their detection possibilities only limited to the characterization of dominant species. The structural elucidation of individual glycolipid structures in complex mixtures extracted from human CNS and their interactions with various proteins at this level [112, 113] is, however, the most important requirement to be fulfilled for assessing the variations in their expression from a CNS region to another or during brain development, maturation and aging since the specificity of these structures in a certain area and at a certain age is related with the specialized function of the respective region and associated with their typical pathologies [114].

A reliable mapping and structural analysis of glycolipids in CNS is highly helpful for understanding the structure and functional interactions of each species involved in pathological processes and for improving their therapeutic potential and usage for early diagnostic. All these aspects determined lately an investment of efforts into the development of superior analytical platforms, among which, those based on mass spectrometry (MS) emerged as the most proficient ones due to the high sensitivity (picomole and subpicomole range), reproducibility and the possibility to provide fragmentation analysis generating detailed information on the glycan core and lipid moiety [110]. Presently, in bioanalytical laboratories, the MS-based methods for the detection and fragmentation of various types of glycolipids, including gangliosides and sulfated glycolipids, are in a continuous progress and improvement.

Nowadays, the most efficient strategies rely on MS equipped with either electrospray ionization (ESI), nano-electrospray (nanoESI) or microfluidics platforms, such as fully automated, robotized chip-based nanoESI coupled with high performance mass analyzers, such as hybrid quadrupole time-of-flight (QTOF), ion traps (IT) and Orbitrap [115–118]. Combining the data acquired by ESI and matrix assisted laser/desorption ionization (MALDI) is also demonstrated as a viable strategy for qualitative, semi-quantitative and in situ analysis of gangliosides, in particular of the species expressed in brain tissue [119].

The modern liquid chromatographic (LC) systems coupled to MS or ion mobility (IMS) MS, providing highly efficient separations of complex mixtures followed by detection

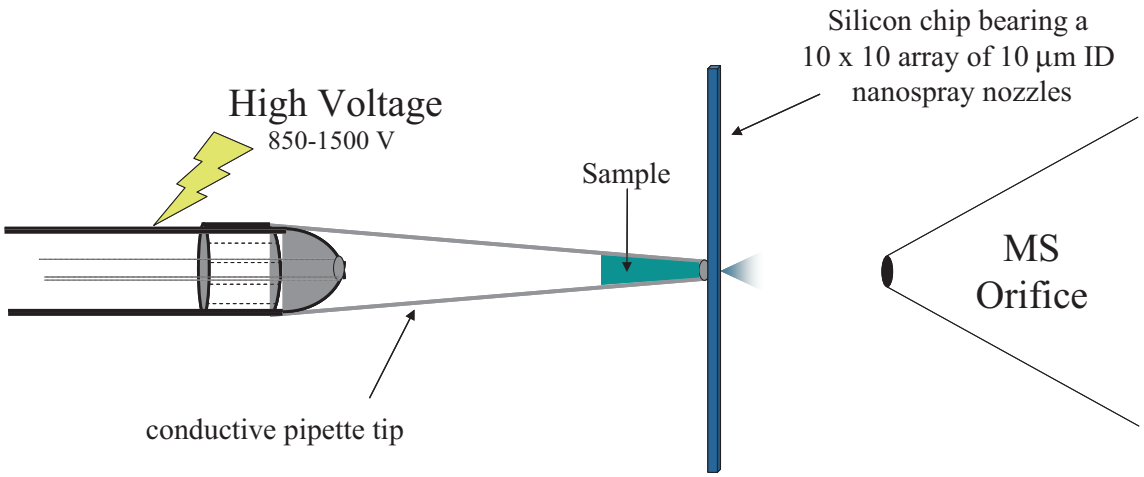

Fig. 42.4 Schematic of chip-based nanoelectrospray setup using a conductive pipette tip and an array of nozzles in a silicon chip

and fragmentation of single components in one and the same MS experiment, represent other resourceful analytical options in glycolipidomics [120]. So far, all these new methods allowed for the first time not only the detection and structural characterization of isolated glycolipid fractions but also a detailed compositional analysis of complex native mixtures extracted from tissues in extremely small amounts (picomolar and attomolar quantities), identification of biomarkers and disease-associated species and their structure elucidation in tandem (MS/MS) or multistage (MS^n) experiments using collision-induced dissociation (CID) at low ion acceleration energies.

The MS methods based on robotized sample delivery by chip-based nanoESI (Fig. 42.4) with automated sample manipulation and delivery in combination with CID MS/MS or even with a total structural analysis by top-down glycolipid fragmentation using CID MS^n is currently performed on the NanoMate robot (produced by Advion BioSciences, Norfolk, UK) in direct coupling with either QTOF, ion trap or Orbitrap MS. This methodology provides numerous advantages: (1) high throughput; (2) several fold sensitivity increase due to the following conjugated benefits: low ESI flows (50–100 nL/min); only 10 µm inner chip diameter; reduction of the sample and reagent consumption, sample handling and potential sample loss; (3) high reproducibility of the experiments due to the 100% reproducibility of the shape of the chip nozzles produced by the most advanced nanotechnology; (4) increased ionization efficiency; (5) high signal-to-noise ratio; (6) mild ionization conditions required, which lead to reduced in-source fragmentation; (7) elimination of cross-contamination and carry-overs from sample to sample.

Often, the robotic chip-based ESI systems with ultrafast CID multistage fragmentations are also combined with automatic mass spectra interpretation using a computer software [121] to yield an integrated high throughput platform (Fig. 42.5). A complex, fully automated system of this type was successfully applied for discovery of ganglioside biomarkers in anencephaly [122]. In a dedicated study, gangliosides were extracted and purified from glial islands of fetal anencephalic brain tissue and investigated in comparison with the gangliosides expressed in normal fetal brain. 25 distinct species in the mixture from anencephalic tissue *vs.* 44 of which 4 asialylated in the normal tissue were discovered. Species such as GT1, GQ1 and GQ2 bearing different ceramide compositions were found biomarkers of anencephaly (Fig. 42.6, Table 42.1) and structurally characterized in details by employing CID MS^n and automatic data interpretation, using an in-house developed software. Moreover, as a general conclusion of the study, the remarkable occurrence of polysialylated structures was considered an effect of brain development stagnation that characterizes anencephaly, which is to be used as a diagnostic of this disease.

Lately, strategies based on LC MS and the modern ultra-performance LC (UPLC) also contributed valuable results to the glycolipidomics field in general and biomarker discovery in particular [120]. Over the past few years, LC MS was optimized and subsequently applied to either glycolipids extracted from tissues, brain in particular, or body fluids such as plasma or CSF. Reverse-phase UPLC/tandem MS method was also validated for such determinations, with excellent results. For instance, in a recent report [123], monosialogangliosides GM1, GM2, and GM3 present in human plasma were separated, identified and structurally characterized by UPLC MS and MS/MS using a methodology that enhanced by 15-fold the MS responses of the analytes by employing 2-(2-Pyridilamino)-ethylamine & 4-(4,6-Dimethoxy-1,3,5-triazin-2-yl)-4-methylmorpholinium chloride-based derivatization. Following the validation, the method could be applied to clinical samples, for monitoring the levels of monosialogangliosides in the plasma of patients suffering from GM3 synthase deficiency.

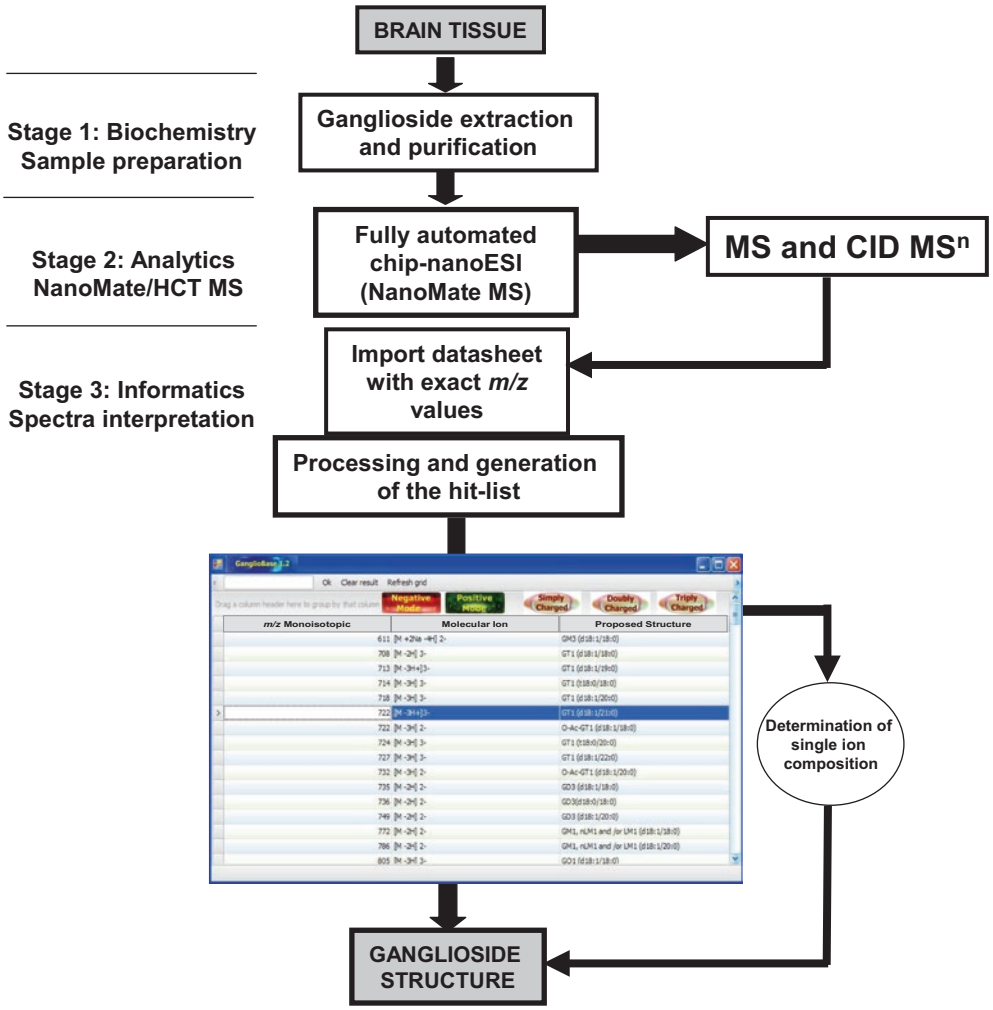

Fig. 42.5 Schematic of the platform for high-throughput ganglioside analysis based on fully automated chip-nanoESI CID MS^n and computer software for automatic interpretation of the mass spectra. Reprint with permission from [121]

The newest analytical technique for MS that has been introduced in glycolipidomics and demonstrated a remarkable potential in glycolipid biomarker discovery is IMS. The method is capable to offer an in-run separation based on the properties of transport driven by the electric field. By IMS MS the ions are separated not only according to the differences in their size, but also in analyte collision cross section, which makes it ideal for discovery of biomarkers and their structural elucidation [124]. IMS MS has the capacity to separate extremely fast and reliably isomers, isobars, and conformers, to reduce the chemical noise and generate data on the stoichiometry, topology and cross section of single biomolecule components in complex native mixtures. Additionally, ions of similar structures and/or charge state are separated into families, displayed along a unique mass-mobility correlation line, which provides a separation into different classes. In combination with efficient fragmentation techniques, IMS MS and MS/MS represents an integrated platform able to: (1) separate the complex mixtures; (2) detect by MS single species in multicomponent samples; (3) provide structural characterization by fragmentation analysis [124].

Although so far mostly developed and applied for proteomics and conformational studies, nucleic acid research and small molecule analysis [125–128], IMS MS in combination with either matrix assisted laser desorption/ionization, MALDI, or ESI or nanoESI MS has shown it effectiveness also in glycolipid research, in particular for discovery and characterization of brain biomarkers [124, 129].

In two dedicated studies conducted using MALDI TOF IMS MS, fractions of mono- to polysialylated brain gangliosides could be separated and characterized in either positive or negative ion mode, with or without a combination of MALDI IMS MS with desorption electrospray ionization [130, 131]. However, recently, ESI QTOF IMS MS and MS/MS was optimized in negative ion mode and introduced in clinical glycolipidomics for mapping of components in highly complex native extracts from normal human brain

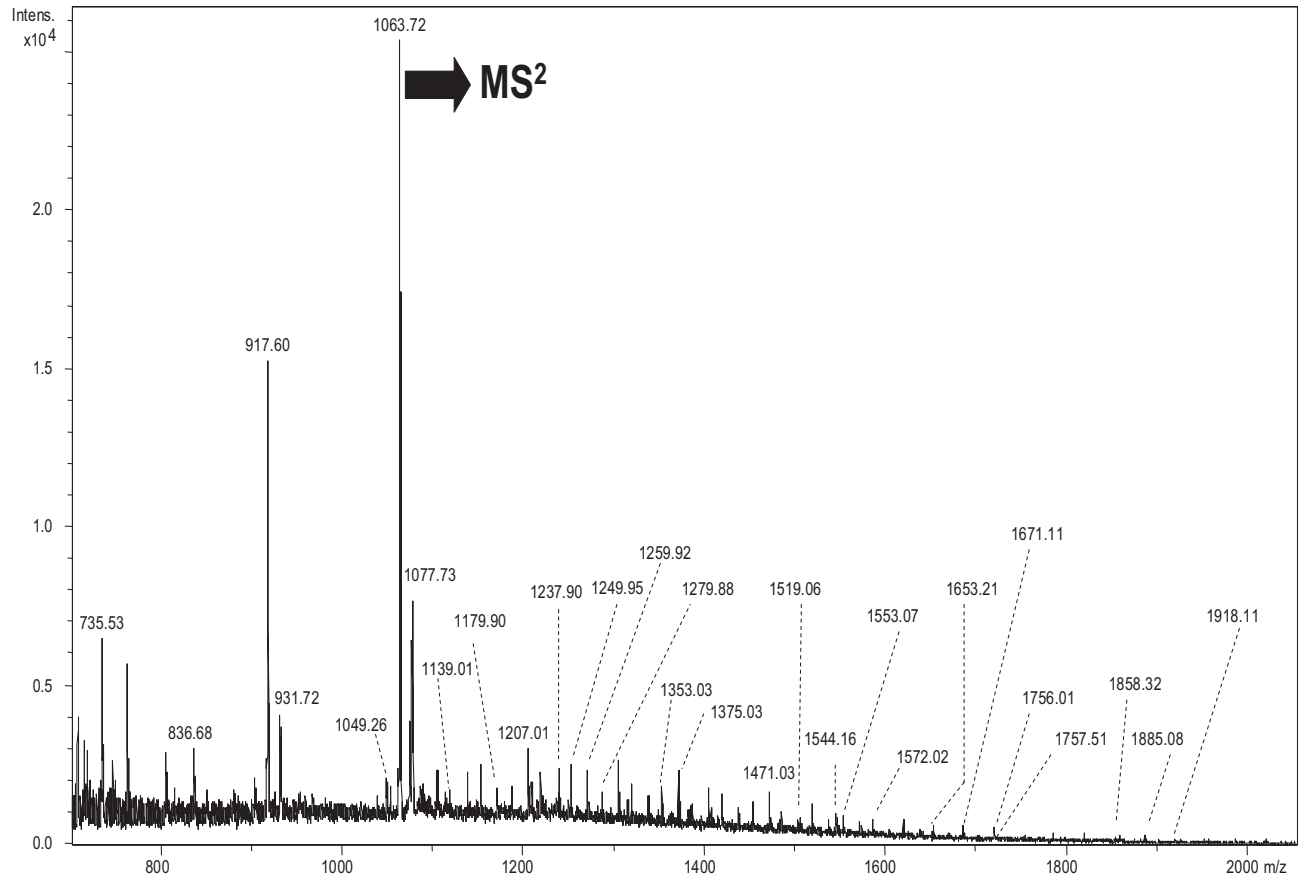

Fig. 42.6 Fully automated chip nanoESI MS in the negative ion mode on a high capacity ion trap of a native ganglioside mixture from glial islands of anencephalic fetus. Solvent: MeOH; sample concentration: 5 pmol/μl; acquisition time: 7 min; chip ESI: 0.8 kV; capillary exit: 50 V. Reprint with permission from [122]

[124]. This method, applied to human fetal frontal lobe, was beneficial for discovery and structural analysis of novel gangliosides associated to healthy human CNS. By ESI IMS MS, no less than 143 distinct structures (Table 42.2) were identified, which represents over three times the number of species detected in fetal frontal lobe by other MS methods. IMS MS results have indicated not only the existence of a larger number of glycoforms or species exhibiting a higher degree of sialylation, but also of an elevated diversity of the ceramide chain than previously discovered in fetal brain (Fig. 42.7a, b). The identification of polysialylated gangliosides, up to GO, octasialoganglioside class, associated to fetal brain is another remarkable achievement of the method, since, prior to IMS MS, pentasialylated species were the gangliosides with the highest Neu5Ac content known to exist in tissues of this origin. Hexa- to octasialylated gangliosides, exhibiting a lower expression, could be for the first time evidenced solely due to the efficient ion mobility separation that allowed discrimination of compounds based on carbohydrate chain length and the number of Neu5Ac residues. Moreover, in the same report, the combination of IMS and CID MS/MS (Fig. 42.8) was shown to offer for the first time detailed structural information upon a novel biomarker species, GalNAc-GQ1 (d18:1/18:0), belonging to the *d* ganglioside series (Fig. 42.9).

Since lipid metabolism has a considerable impact in neurodegeneration, advanced mass spectrometry with or without liquid-based separation methods prior to mass detection and species identification was also intensively involved in discovery of glycolipids associated to different types of neurodegenerative disorders, such as PD and various forms of dementia, in particular AD.

In the AD case, the major neuropathologic hallmarks in the brain are extracellular plaques of aggregated Aβ protein and intracellular neurofibrillary tangles (NFT) containing hyperphosphorylated tau protein, accompanied by a profound loss of basal forebrain cholinergic neurons that innervate the hippocampus and the neocortex. The conversion of nontoxic, soluble Aβ monomer to its toxic aggregates is considered to be the key step in AD development, though the mechanism is still obscure. The Aβ plaques are most prominent in areas affected by neurodegeneration, such as the entorhinal cortex, hippocampus and association cortices [132, 133]. Brain, among all other organs, contains the highest ganglioside con-

Table 42.1 Assignment of the major ions detected by chip-based nanoESI MS screening in the negative ion mode of the native ganglioside mixture extracted from glial islands of anencephalic fetus

m/z Experimental	Molecular ion	Proposed structure
735.53	$[M - 2H]^{2-}$	GD3(d18:0/18:0)
836.68	$[M - 2H]^{2-}$	GD2(d18:1/18:0)
917.60	$[M - 2H]^{2-}$	GD1(d18:1/18:0)
931.72	$[M - 2H]^{2-}$	GD1(18:1/20:0)
1049.26	$[M - 2H]^{2-}$	GT1(18:1/16:0)
1063.72	$[M - 2H]^{2-}$	GT1(d18:1/18:0)
1077.73	$[M - 2H]^{2-}$	GT1(d18:1/20:0)
1139.01	$[M - H]^{-}$	GM3(d18:1/14:0) or (d18:1/h14:0) or $HexNAcHex_2Cer$ (d18:1/22:4)
1179.90	$[M - H]^{-}$	GM3 (d18:1/18:0)
1207.01	$[M - H]^{-}$	GM3(d18:1/20:0)
1237.90	$[M - H]^{-}$	GM3 (d18:0/22:0)
1249.95	$[M - H]^{-}$	*O*-Ac-GM3 (d18:1/20:0) or GM3 (18:1/23:0)
1259.92	$[M - H]^{-}$	GM3 (d18:1/24:2)
1279.88	$[M - H]^{-}$	*O*-Ac-GM3 (d18:0/22:0) or GM3 (20:0/23:0)
1353.03	$[M - H]^{-}$	GM2 (d18:1/16:0)
1354.79	$[M - H]^{-}$	GM2 (d18:1/16:0)
1471.03	$[M - H]^{-}$	GD3(d18:1/18:0)
1472.79	$[M - H]^{-}$	GD3 (d18:0/18:0)
1519.06	$[M - H]^{-}$	GM1, nLM1 and/or LM1 (d18:0/16:0)
1544.16	$[M - H]^{-}$	GM1, nLM1 and/or LM1 (d18:1/18:0)
1553.07	$[M - H]^{-}$	GD3(d18:1/24:1)
1572.02	$[M - H]^{-}$	GM1, nLM1 and/or LM1 (d18:0/20:0)
1845.01	$[M - H]^{-}$	GT3(d18:1/24:0)
1858.32	$[M + Na - 2H]^{-}$	GD1(d18:0/18:0)
1885.08	$[M - H]^{-}$	GT3(d18:1/24:1)
2256.50	$[M - H]^{-}$	GQ2(d18:1/18:0)
2417.45	$[M - H]^{-}$	GQ1(d18:1/18:0)

Reprint with permission from [122]

centration, which is particularly high in neuronal membranes in the synapses. Hence, gangliosides, especially GM1, were shown to have neuritogenic and neuronotrophic activity and to facilitate repair of neuronal tissue after mechanical, biochemical or toxic injuries. Continuous intracerebroventricular infusion of GM1 was demonstrated for long time [134] to have a significant beneficial effect in patients with an early onset AD (AD Type I). Moreover, the peripheral treatment of AD mutant mice, by intraperitoneal administration with GM1, having a high affinity for Aβ, resulted in the reduction of Aβ level in the brain, suggesting that GM1 might serve as a therapeutic agent, reducing and preventing brain amyloidosis by sequestering the plasma Aβ. On the other hand, already more than a decade ago, interactions of Aβ (1–40) with ganglioside-containing membranes, particularly with membrane rafts enriched in GM1 and GM2, have been hypothesized to be involved in the pathogenesis of AD [135].

Using conventional high performance thin-layer chromatographic separation/detection, immunochemical and immunohistochemical detection methods, some remarkable studies [136, 137] have described the specific role and/or changes in ganglioside expression and quantity in investigated regions of human brains diagnosed with AD disease. However, several modern and highly efficient methods and innovative protocols based on either LC MS [138], as comprehensively reviewed by Touboul and Gaudin, [139] or imaging MS were developed for lipid and glycolipid profiling and structural analysis in either post-mortem AD brain specimens or in plasma of diagnosed patients, followed by identification of species associated to the disease.

An interesting example illustrating the efficacy of LC MS method is the work of Oikawa's group [140]. In 2015, by liquid chromatography coupled to MS, the authors have measured and observed an increase in the ratio of the level of GD1b-ganglioside containing C20:0 fatty acid to that containing C18:0 in specimens of precuneus and calcarine cortex from human brains neuropathologically classified and diagnosed with AD. The findings were postulated as a cause of the enhanced Aβ assembly in the precuneus. From the clinical point of view, the accurate data obtained by the employed LC MS protocol demonstrated clearly that the local glycolipid surrounding plays a critical role in the initiation of Alzheimer amyloid deposition.

Focused mostly on the ceramide role, Jung and collaborators [141] have discovered by LC MS/MS that C2 ceramide, rather than the modified ceramide-1-phosphate or long chain ceramides mainly function by penetrating into the microglial cells and exerts anti-inflammatory effects. Such results certainly suggest the therapeutic potential of species exhibiting short chain ceramides, such as C2 for neuroinflammatory disorders like Alzheimer's and Parkinson's disease.

On the other hand, MALDI imaging MS was demonstrated as an invaluable tool for assessing the expression and levels of monosialylated GM2 and GM3 type gangliosides in a combined rat model of Aβ toxicity and stroke. In the study by Caughlin et al. [142], MALDI imaging MS tuned in the negative ion mode has revealed for the first time a modification in ganglioside composition in stroke and a different alteration of their expression when Aβ toxicity was present as a comorbidity. From the clinical point of view, these findings are the first to suggest that a synergic molecular mechanism might be involved in brains affected by AD and stroke comorbidities.

The mechanism of dysfunction that occurs in AD was also approached by imaging mass spectrometry, considering the spatial arrangement of monosialotetraose (GM1) expressed in hippocampus, the region strongly affected by the disease. Hence, by imaging MS, the group of Hirano-Sakamaki [60] discovered an interesting decrease in the ratio of GM1(20:1/18:0)/ GM1(18:1/18:0) in the outer molecular

Table 42.2 Assignment of the major ions detected by IMS MS screening in the negative ion mode of the native ganglioside mixture extracted from normal human fetal brain

No. crt.	*m/z* Experimental	*m/z* Theoretical	Mass accuracy (ppm)	Proposed structure	Molecular ion
1	477.608	477.611	6.289	GM2 (d18:1/22:2)	$[M - 3H^+]^{3-}$
2	498.274	498.277	6.024	GD3 (d18:1/20:1)	$[M - 3H^+]^{3-}$
3	502.293	502.289	7.968	GD3 (d18:1/22:0)	$[M - H_2O - 3H^+]^{3-}$
4	526.301	526.297	7.605	GM1 (d18:1/22:1)	$[M - H_2O - 3H^+]^{3-}$
5	531.014	531.009	9.416	GT1 (d18:1/18:0)	$[M - 4H^+]^{4-}$
6	545.029	545.025	7.339	GT1 (d18:1/22:0)	$[M - 4H^+]^{4-}$
7	546.971	546.975	7.326	*O*-Ac-GM1 (d18:1/22:0)	$[M - 3H^+]^{3-}$
8	551.021	551.025	7.260	GT1 (d18:1/24:2)	$[M - 4H^+]^{4-}$
9	555.027	555.023	7.207	GT1 (t18:1/24:2)	$[M - 4H^+]^{4-}$
10	559.291	559.295	7.156	GD2 (d18:1/20:2)	$[M - H_2O - 3H^+]^{3-}$
11	563.949	563.954	8.881	GD2 (d18:1/18:1)	$[M - H_2O - 4H^+ + Na^+]^{3-}$
12	574.974	574.982	13.937	Fuc-GM1 (d18:1/22:1)	$[M - H_2O - 3H^+]^{3-}$
13	586.635	586.637	3.413	GT3 (t18:0/18:0)	$[M - H_2O - 3H^+]^{3-}$
14	595.972	595.981	15.126	GT3 (t18:0/20:0)	$[M - H_2O - 3H^+]^{3-}$
15	596.770	596.775	8.389	GQ1 (d18:1/16:0)	$[M - 4H^+]^{4-}$
16	600.637	600.641	6.667	GT3 (t18:1/20:1)	$[M - 3H^+]^{3-}$
17	603.778	603.783	8.292	GQ1 (d18:1/18:0)	$[M - 4H^+]^{4-}$
18	610.784	610.791	11.475	GQ1 (d18:1/20:0)	$[M - 4H^+]^{4-}$
19	611.310	611.316	9.819	GD1 (d18:1/18:0)	$[M - 3H^+]^{3-}$
20	613.987	613.997	16.313	GT3 (d18:1/24:1)	$[M - 3H^+]^{3-}$
21	613.805	613.800	8.157	GQ1 (d18:0/22:0)	$[M - H_2O - 4H^+]^{4-}$
22	617.793	617.799	9.724	GQ1 (d18:1/22:0)	$[M - 4H^+]^{4-}$
23	621.327	621.332	8.052	GD1 (d18:0/20:0)	$[M - 3H^+]^{3-}$
24	624.296	624.302	9.615	GQ1 (d18:1/24:1)	$[M - 4H^+]^{4-}$
25	637.960	637.967	10.989	Fuc-GT3 (t18:1/16:1)	$[M - 4H^+ + Na^+]^{3-}$
26	644.383	644.388	7.764	GM3 (d18:1/24:0)	$[M - H_2O - 4H^+ + 2Na^+]^{2-}$
27	674.867	674.873	8.902	GM2 (d18:1/16:2)	$[M - 2H^+]^{2-}$
28	676.551	676.557	8.876	GP1 (d18:1/18:0)	$[M - 4H^+]^{4-}$
29	683.65	683.657	10.249	GT1 (d18:1/14:0)	$[M - H_2O - 3H^+]^{3-}$
30	689.649	689.660	15.965	GT1 (d18:1/14:0)	$[M - 3H^+]^{3-}$
31	698.998	699.004	8.584	GT1 (d18:1/16:0)	$[M - 3H^+]^{3-}$
32	707.668	707.676	11.315	GT1 (d18:1/18:1)	$[M - 3H^+]^{3-}$
33	707.921	707.914	9.901	GM2 (d18:1/22:2)	$[M - H_2O - 2H^+]^{2-}$
34	708.338	708.348	14.124	GT1 (d18:1/18:0)	$[M - 3H^+]^{3-}$
35	713.002	713.008	8.415	GT1 (t18:1/18:1)	$[M - 3H^+]^{3-}$
36	713.666	713.659	9.818	GT1 (d18:1/16:0)	$[M - 5H^+ + 2Na^+]^{3-}$
37	714.339	714.351	16.806	GT1 (t18:0/18:0)	$[M - 3H^+]^{3-}$
38	717.013	717.020	9.763	GT1 (d18:1/20:1)	$[M - 3H^+]^{3-}$
39	717.681	717.692	15.342	GT1 (d18:1/20:0)	$[M - 3H^+]^{3-}$
40	716.927	716.920	9.777	GM2 (d18:1/22:2)	$[M - 2H^+]^{2-}$
41	720.889	720.896	9.722	GD3 (d18:1/16:0)	$[M - 2H^+]^{2-}$
42	722.345	722.352	9.695	GT1 (t18:1/20:1)	$[M - 3H^+]^{3-}$
43	726.359	726.363	6.887	GT1 (d18:1/22:1)	$[M - 3H^+]^{3-}$
44	727.023	727.036	17.881	GT1 (d18:1/22:0)	$[M - 3H^+]^{3-}$
45	731.688	731.695	9.576	GT1 (t18:1/22:1)	$[M - 3H^+]^{3-}$
46	733.893	733.904	15.007	GD3 (d18:1/18:1)	$[M - 2H^+]^{2-}$
47	734.905	734.912	9.537	GD3 (d18:1/18:0)	$[M - 2H^+]^{2-}$
48	735.026	735.035	12.244	*O*-Ac-GT1 (d18:1/22:0)	$[M - H_2O - 3H^+]^{3-}$
49	735.699	735.707	10.884	*O*-Ac-GT1 (d18:0/22:0)	$[M - H_2O - 3H^+]^{3-}$
50	748.921	748.928	9.358	GD3 (d18:1/20:0)	$[M - 2H^+]^{2-}$
51	762.937	762.943	7.874	GD3 (d18:1/22:0)	$[M - 2H^+]^{2-}$
52	771.942	771.949	9.079	GD3 (t18:0/22:0)	$[M - 2H^+]^{2-}$
53	775.730	775.722	10.323	Fuc-GT1 (d18:1/22:0)	$[M - 3H^+]^{3-}$
54	775.944	775.951	9.032	GD3 (d18:1/24:1)	$[M - 2H^+]^{2-}$
55	781.717	781.725	10.243	Fuc-GT1 (t18:0/22:0)	$[M - 3H^+]^{3-}$

(continued)

Table 42.2 (continued)

No. crt.	*m/z* Experimental	*m/z* Theoretical	Mass accuracy (ppm)	Proposed structure	Molecular ion
56	794.013	794.020	8.816	GQ1 (d18:1/16:3)	$[M - 3H^+]^{3-}$
57	796.029	796.036	8.794	GQ1 (d18:1/16:0)	$[M - 3H^+]^{3-}$
58	804.695	804.708	16.169	GQ1 (d18:1/18:1)	$[M - 3H^+]^{3-}$
59	806.943	806.951	9.926	*O*-Ac GM1 (d18:1/20:0)	$[M - 2H^+]^{2-}$
60	811.941	811.949	9.864	GD3 (d18:1/26:1)	$[M - 4H^+ + 2Na^+]^{2-}$
61	812.699	812.707	9.852	GQ1 (d18:1/18:0)	$[M - 4H^+ + Na^+]^{3-}$
62	814.716	814.724	9.828	GQ1 (d18:1/20:0)	$[M - 3H^+]^{3-}$
63	819.373	819.383	12.210	*O*-Ac-GQ1 (d18:1/18:0)	$[M - 3H^+]^{3-}$
64	824.035	824.043	9.709	*O*-Ac-GQ1 (t18:1/18:1)	$[M - 3H^+]^{3-}$
65	832.731	832.739	9.615	GQ1 (t18:1/24:0)	$[M - H_2O - 3H^+]^{3-}$
66	835.435	835.444	10.778	GD2 (d18:1/18:1)	$[M - 2H^+]^{2-}$
67	836.445	836.452	8.373	GD2 (d18:1/18:0)	$[M - 2H^+]^{2-}$
68	850.459	850.467	9.412	GD2 (d18:1/20:0)	$[M - 2H^+]^{2-}$
69	889.456	889.465	10.124	GT3 (t18:0/18:0)	$[M - 2H^+]^{2-}$
70	894.466	894.475	10.067	GT3 (t18:0/20:0)	$[M - H_2O - 2H^+]^{2-}$
71	902.403	902.412	9.978	GP1 (d18:1/18:0)	$[M - 3H^+]^{3-}$
72	903.472	903.462	11.074	GD1 (d18:1/16:0)	$[M - 2H^+]^{2-}$
		903.481	9.967	GT3 (t18:0/20:0)	$[M - 2H^+]^{2-}$
73	908.463	908.473	11.013	GD1 (d18:1/18:0)	$[M - H_2O - 2H^+]^{2-}$
74	916.461	916.470	9.825	GD1 (d18:1/18:1)	$[M - 2H^+]^{2-}$
75	917.468	917.478	10.905	GD1 (d18:1/18:0)	$[M - 2H^+]^{2-}$
76	923.509	923.515	6.501	GT3 (d18:0/24:0)	$[M - 2H^+]^{2-}$
77	930.465	930.486	22.580	GD1 (d18:1/20:1)	$[M - 2H^+]^{2-}$
		930.474	9.677	*O*-Ac GT3 (d18:1/22:1)	$[M - H_2O - 3H^+ + Na^+]^{2-}$
78	931.475	931.494	20.408	GD1 (d18:1/20:0)	$[M - 2H^+]^{2-}$
		931.482	7.518	*O*-Ac GT3 (d18:1/22:0)	$[M - H_2O - 3H^+ + Na^+]^{2-}$
79	944.481	944.501	21.186	GD1 (d18:1/22:1)	$[M - 2H^+]^{2-}$
		944.490	9.534	*O*-Ac GT3 (d18:1/24:1)	$[M - H_2O - 3H^+ + Na^+]^{2-}$
80	945.488		23.280	GD1 (d18:1/22:0)	$[M - 2H^+]^{2-}$
		945.498	945.510	*O*-Ac GT3 (d18:1/24:0)	$[M - H_2O - 3H^+ + Na^+]^{2-}$
81	951.481	951.491	10.515	*O*-Ac GD1 (d18:1/20:1)	$[M - 2H^+]^{2-}$
82	952.489	952.499	10.504	*O*-Ac GD1 (d18:1/20:0)	$[M - 2H^+]^{2-}$
83	957.446	957.454	8.359	Fuc-GT3 (t18:1/16:1)	$[M - 3H^+ + Na^+]^{2-}$
84	958.453	958.462	9.395	Fuc-GT3 (t18:1/16:0)	$[M - 3H^+ + Na^+]^{3-}$
85	966.507	966.497	10.351	Fuc-GT3 (d18:1/20:1)	$[M - 2H^+]^{2-}$
		966.514	7.246	*O*-Ac GD1 (d18:1/22:0)	$[M - 2H^+]^{2-}$
86	967.512	967.504	8.273	Fuc-GT3 (d18:1/20:0)	$[M - 2H^+]^{2-}$
		967.522	10.341	*O*-Ac GD1 (d18:0/22:0)	$[M - 2H^+]^{2-}$
87	972.464	972.477	13.374	Fuc-GT3 (t18:1/18:0)	$[M - 2H^+]^{2-}$
88	980.502	980.512	10.204	Fuc-GT3 (d18:1/22:1)	$[M - 2H^+]^{2-}$
89	988.482	988.492	10.121	Fuc-GD1 (d18:1/18:2)	$[M - 2H^+]^{2-}$
90	989.489	989.499	10.111	Fuc-GD1 (d18:1/18:1)	$[M - 2H^+]^{2-}$
91	990.497	990.507	10.101	Fuc-GD1 (d18:1/18:0)	$[M - 2H^+]^{2-}$
92	991.503	991.515	12.109	Fuc-GD1 (d18:0/18:0)	$[M - 2H^+]^{2-}$
93	992.502	992.512	10.081	Fuc-GT3 (d18:1/24:3)	$[M - 2H^+]^{2-}$
94	1017.941	1017.955	13.675	GT1 (d18:1/12:3)	$[M - 2H^+]^{2-}$
95	1018.952	1018.963	10.806	GT1 (d18:1/12:2)	$[M - 2H^+]^{2-}$
96	1027.958	1027.969	10.711	GT1 (t18:1/12:1)	$[M - 2H^+]^{2-}$
97	1032.969	1032.979	9.689	GT1 (d18:1/14:2)	$[M - 2H^+]^{2-}$
98	1038.948	1038.960	11.561	GT1 (t18:1/12:1)	$[M - 3H^+ + Na^+]^{2-}$
99	1044.967	1044.978	10.536	GT1 (d18:1/14:1)	$[M - 3H^+ + Na^+]^{2-}$
100	1048.998	1049.010	11.439	GT1 (d18:1/16:0)	$[M - 2H^+]^{2-}$
101	1050.985	1050.996	10.476	GT1 (d18:1/16:0)	$[M - H_2O - 3H^+ + Na^+]^{2-}$
102	1059.991	1060.001	9.434	GT1 (d18:1/16:0)	$[M - 3H^+ + Na^+]^{2-}$
103	1060.998	1061.010	11.310	GT1 (d18:1/18:2)	$[M - 2H^+]^{2-}$

(continued)

Table 42.2 (continued)

No. crt.	*m/z* Experimental	*m/z* Theoretical	Mass accuracy (ppm)	Proposed structure	Molecular ion
104	1062.009	1062.018	8.475	GT1 (d18:1/18:1)	$[M - 2H^+]^{2-}$
105	1063.015	1063.026	10.348	GT1 (d18:1/18:0)	$[M - 2H^+]^{2-}$
106	1074.007	1074.018	10.242	GT1 (d18:1/20:3)	$[M - 2H^+]^{2-}$
		1074.017	9.310	GT1 (d18:1/18:0)	$[M - 3H^+ + Na^+]^{2-}$
107	1077.031	1077.042	10.214	GT1 (d18:1/20:0)	$[M - 2H^+]^{2-}$
108	1084.018	1084.031	11.993	GT1 (t18:1/20:1)	$[M - 2H^+]^{2-}$
109	1088.022	1088.034	11.029	GT1 (d18:1/22:3)	$[M - 2H^+]^{2-}$
110	1091.043	1091.057	12.832	GT1 (d18:1/22:0)	$[M - 2H^+]^{2-}$
111	1100.051	1100.063	10.909	GT1 (t18:0/22:0)	$[M - 2H^+]^{2-}$
112	1104.051	1104.065	12.681	GT1 (d18:1/24:1)	$[M - 2H^+]^{2-}$
113	1115.042	1115.056	12.556	GT1 (d18:1/24:1)	$[M - 3H^+ + Na^+]^{2-}$
114	1125.813	1125.805	7.111	GS1 (t18:1/20:0)	$[M - 5H^+ + 2Na^+]^{3-}$
115	1126.472	1126.477	4.440	GS1 (t18:0/20:0)	$[M - 5H^+ + 2Na^+]^{3-}$
116	1135.151	1135.149	1.762	GS1 (t18:1/22:0)	$[M - 5H^+ + 2Na^+]^{3-}$
117	1135.828	1135.821	6.167	GS1 (t18:0/22:0)	$[M - 5H^+ + 2Na^+]^{3-}$
118	1165.081	1165.094	11.159	Fuc-GT1 (d18:0/22:0)	$[M - 2H^+]^{2-}$
119	1169.497	1169.500	2.566	GalNAc-GS1 (t18:1/18:0)	$[M - 3H^+]^{3-}$
120	1176.826	1176.827	0.850	GalNAc-GS1 (t18:1/18:0)	$[M - 4H^+ + Na^+]^{3-}$
121	1177.726	1177.721	4.24	GM3 (d18:1/18:1)	$[M - H^+]^-$
122	1179.087	1179.110	19.508	Fuc-GT1 (d18:0/24:0)	$[M - 2H^+]^{2-}$
123	1179.724	1179.737	11.026	GM3 (d18:1/18:0)	$[M - H^+]^-$
124	1194.162	1194.171	7.538	GalNAc-GS1 (t18:1/22:2)	$[M - 4H^+ + Na^+]^{3-}$
125	1207.553	1207.566	10.771	GQ1 (d18:1/18:1)	$[M - 2H^+]^{2-}$
126	1208.560	1208.574	11.589	GQ1 (d18:1/18:0)	$[M - 2H^+]^{2-}$
127	1214.150	1214.165	12.356	GO1 (t18:0/18:0)	$[M - 5H^+ + 2Na^+]^{3-}$
128	1218.543	1218.557	11.494	GQ1 (d18:1/18:1)	$[M - 3H^+ + Na^+]^{2-}$
129	1219.551	1219.565	11.485	GQ1 (d18:1/18:0)	$[M - 3H^+ + Na^+]^{2-}$
130	1222.574	1222.589	12.275	GQ1 (d18:1/20:0)	$[M - 2H^+]^{2-}$
131	1222.823	1222.837	11.457	GO1 (t18:1/20:0)	$[M - 5H^+ + 2Na^+]^{3-}$
132	1229.561	1229.579	14.646	*O*-Ac GQ1 (d18:1/18:0)	$[M - 2H^+]^{2-}$
133	1230.149	1230.164	12.195	GO1 (t18:1/20:0)	$[M - 6H^+ + 3Na^+]^{3-}$
134	1232.837	1232.853	12.987	GO1 (t18:0/22:0)	$[M - 5H^+ + 2Na^+]^{3-}$
135	1236.579	1236.605	21.036	GQ1 (d18:1/22:0)	$[M - 2H^+]^{2-}$
136	1239.494	1239.508	11.299	GO1 (t18:1/22:0)	$[M - 6H^+ + 3Na^+]^{3-}$
137	1248.844	1248.852	6.410	GO1 (t18:1/24:0)	$[M - 6H^+ + 3Na^+]^{3-}$
138	1249.598	1249.613	12.009	GQ1 (t18:1/24:0)	$[M - H_2O - 2H^+]^{2-}$
139	1310.128	1310.113	11.450	GalNAc-GQ1 (d18:1/18:0)	$[M - 2H^+]^{2-}$
140	1321.121	1320.104	12.648	GalNAc-GQ1 (d18:1/18:0)	$[M - 3H^+ + Na^+]^{2-}$
141	1350.770	1350.753	12.592	GM2 (d18:1/16:2)	$[M - H^+]^-$
142	1354.768	1354.785	12.555	GM2 (d18:1/16:0)	$[M - H^+]^-$
143	1380.782	1380.800	13.043	GM2 (d18:1/18:1)	$[M - H^+]^-$
144	1382.797	1382.816	13.748	GM2 (d18:1/18:0)	$[M - H^+]^-$
145	1410.826	1410.847	14.894	GM2 (d18:1/20:0)	$[M - H^+]^-$
146	1438.858	1438.879	14.604	GM2 (d18:1/22:0)	$[M - H^+]^-$
147	1440.767	1440.785	12.500	GD3 (d18:1/16:1)	$[M - H^+]^-$
148	1442.783	1442.801	12.482	GD3 (d18:1/16:0)	$[M - H^+]^-$
149	1463.639	1463.658	12.987	GalNAc-GP1 (t18:1/18:0)	$[M - 2H^+]^{2-}$
150	1468.820	1468.816	2.724	GD3 (d18:1/18:1)	$[M - H^+]^-$
151	1470.813	1470.832	12.925	GD3 (d18:1/18:0)	$[M - H^+]^-$
152	1498.844	1498.863	12.684	GD3 (d18:1/20:0)	$[M - H^+]^-$
153	1507.646	1507.667	13.935	GH1 (t18:1/18:0)	$[M - 2H^+]^{2-}$
154	1516.817	1516.838	13.852	GM1 (d18:1/16:0)	$[M - H^+]^-$
155	1518.636	1518.657	13.834	GH1 (t18:1/18:0)	$[M - 3H^+ + Na^+]^{2-}$
156	1526.876	1526.895	12.451	GD3 (d18:1/22:0)	$[M - H^+]^-$
157	1542.869	1542.853	10.376	GM1 (d18:1/18:1)	$[M - H^+]^-$
		1542.890	13.619	GD3 (t18:1/22:0)	$[M - H^+]^-$

(continued)

Table 42.2 (continued)

No. crt.	*m/z* Experimental	*m/z* Theoretical	Mass accuracy (ppm)	Proposed structure	Molecular ion
158	1543.641	1543.664	14.906	GH1 (t18:1/20:0)	$[M - 4H^+ + 2Na^+]^{2-}$
159	1544.649	1544.672	14.896	GH1 (t18:0/20:0)	$[M - 4H^+ + 2Na^+]^{2-}$
160	1544.849	1544.869	12.953	GM1 (d18:1/18:0)	$[M - H^+]^-$
161	1552.884	1552.910	16.753	GD3 (d18:1/24:1)	$[M - H^+]^-$
162	1558.826	1558.848	14.121	*O*-Ac GM1 (d18:1/16:0)	$[M - H^+]^-$
163	1570.901	1570.884	10.828	GM1 (d18:1/20:1)	$[M - H^+]^-$
		1570.921	12.739	GD3 (t18:1/24:0)	$[M - H^+]^-$
164	1572.917	1572.900	10.814	GM1 (d18:1/20:0)	$[M - H^+]^-$
		1572.937	12.723	GD3 (t18:0/24:0)	$[M - H^+]^-$
165	1586.857	1586.879	13.871	*O*-Ac GM1 (d18:1/18:0)	$[M - H^+]^-$
166	1598.893	1598.916	14.393	GM1 (d18:1/22:1)	$[M - H^+]^-$
167	1600.920	1600.931	6.875	GM1 (d18:1/22:0)	$[M - H^+]^-$
168	1609.185	1609.206	13.052	GalNAc-GH1 (t18:1/18:0)	$[M - 2H^+]^{2-}$
169	1620.172	1620.197	15.432	GalNAc-GH1 (t18:1/18:0)	$[M - 3H^+ + Na^+]^{2-}$
170	1623.198	1623.222	14.787	GalNAc-GH1 (t18:1/20:0)	$[M - 2H^+]^{2-}$
171	1624.915	1624.931	9.852	GM1 (d18:1/24:2)	$[M - 2H^+]^{2-}$
		1624.905	6.157	GD3 (d18:1/26:1)	$[M - 3H^+ + 2Na^+]^{2-}$
172	1626.929	1626.947	11.070	GM1 (d18:1/24:1)	$[M - 2H^+]^{2-}$
		1626.921	4.92	GD3 (d18:1/26:0)	$[M - 3H^+ + 2Na^+]^{2-}$
173	1640.962	1640.963	0.609	*O*-Ac-GD3 (t18:1/26:0)	$[M - H^+]^-$
174	1671.873	1671.896	13.764	GD2 (d18:1/18:1)	$[M - H^+]^-$
175	1673.878	1673.911	19.725	GD2 (d18:1/18:0)	$[M - H^+]^-$
176	1675.172	1675.196	14.328	GS1 (t18:1/18:0)	$[M - 4H^+ + 2Na^+]^{2-}$
177	1689.187	1689.212	14.802	GS1 (t18:1/20:0)	$[M - 4H^+ + 2Na^+]^{2-}$
178	1690.903	1690.927	14.201	Fuc-GM1 (d18:1/18:0)	$[M - H^+]^-$
179	1700.177	1700.203	15.294	GS1 (t18:1/20:0)	$[M - 5H^+ + 3Na^+]^{2-}$
180	1701.920	1701.943	13.521	GD2 (d18:1/20:0)	$[M - H^+]^-$
181	1714.193	1714.218	14.585	GS1 (t18:1/22:0)	$[M - 5H^+ + 3Na^+]^{2-}$
182	1754.729	1754.754	14.253	GalNAc-GS1 (t18:1/18:0)	$[M - 2H^+]^{2-}$
183	1765.720	1765.745	14.164	GalNAc-GS1 (t18:1/18:0)	$[M - 3H^+ + Na^+]^{2-}$
184	1776.708	1776.736	15.766	GalNAc-GS1 (t18:1/18:0)	$[M - 4H^+ + 2Na^+]^{2-}$
185	1790.727	1790.752	13.966	GalNAc-GS1 (t18:1/20:0)	$[M - 4H^+ + 2Na^+]^{2-}$
186	1807.896	1807.933	20.476	GD1 (d18:1/16:0)	$[M - H^+]^-$
187	1833.922	1833.949	14.729	GD1 (d18:1/18:1)	$[M - H^+]^-$
188	1834.737	1834.760	12.541	GO1 (t18:1/20:0)	$[M - 4H^+ + 2Na^+]^{2-}$
189	1835.937	1835.964	14.714	GD1 (d18:1/18:0)	$[M - H^+]^-$
190	1835.739	1835.767	15.259	GO1 (t18:0/20:0)	$[M - 4H^+ + 2Na^+]^{2-}$
191	1845.725	1845.751	14.092	GO1 (t18:1/20:0)	$[M - 5H^+ + 3Na^+]^{2-}$
192	1846.729	1846.758	15.709	GO1 (t18:0/20:0)	$[M - 5H^+ + 3Na^+]^{2-}$
193	1856.714	1856.741	14.547	GO1 (t18:1/20:0)	$[M - 6H^+ + 4Na^+]^{2-}$
194	1857.721	1857.749	15.078	GO1 (t18:0/20:0)	$[M - 6H^+ + 4Na^+]^{2-}$
195	1857.919	1857.946	14.539	GD1 (d18:1/18:0)	$[M - 2H^+ + Na^+]^-$
196	1860.748	1860.774	13.978	GO1 (t18:0/22:0)	$[M - 2H^+ + Na^+]^-$
197	1863.967	1863.996	15.566	GD1 (d18:1/20:0)	$[M - H^+]^-$
198	1871.735	1871.765	16.034	GO1 (t18:0/22:0)	$[M - 6H^+ + 4Na^+]^{2-}$
199	1877.948	1877.975	14.385	GD1 (t18:1/20:1)	$[M - H^+]^-$
200	1885.752	1885.781	15.384	GO1 (t18:0/24:0)	$[M - 6H^+ + 4Na^+]^{2-}$
201	1885.989	1885.977	6.366	GD1 (d18:1/20:0)	$[M - 2H^+ + Na^+]^-$
		1885.980	4.774	GD1 (d18:1/22:3)	$[M - H^+]^-$
		1886.016	14.316	*O*-Ac GT3 (d18:1/24:1)	$[M - H^+]^-$
202	1889.993	1889.949	23.292	GD1 (d18:1/20:0)	$[M - H_2O - 3H^+ + 2Na^+]^-$
		1890.011	9.528	GD1 (d18:1/22:1)	$[M - H^+]^-$
		1890.048	29.115	*O*-Ac GT3 (d18:0/24:0)	$[M - H^+]^-$

Reprint with permission from [124]

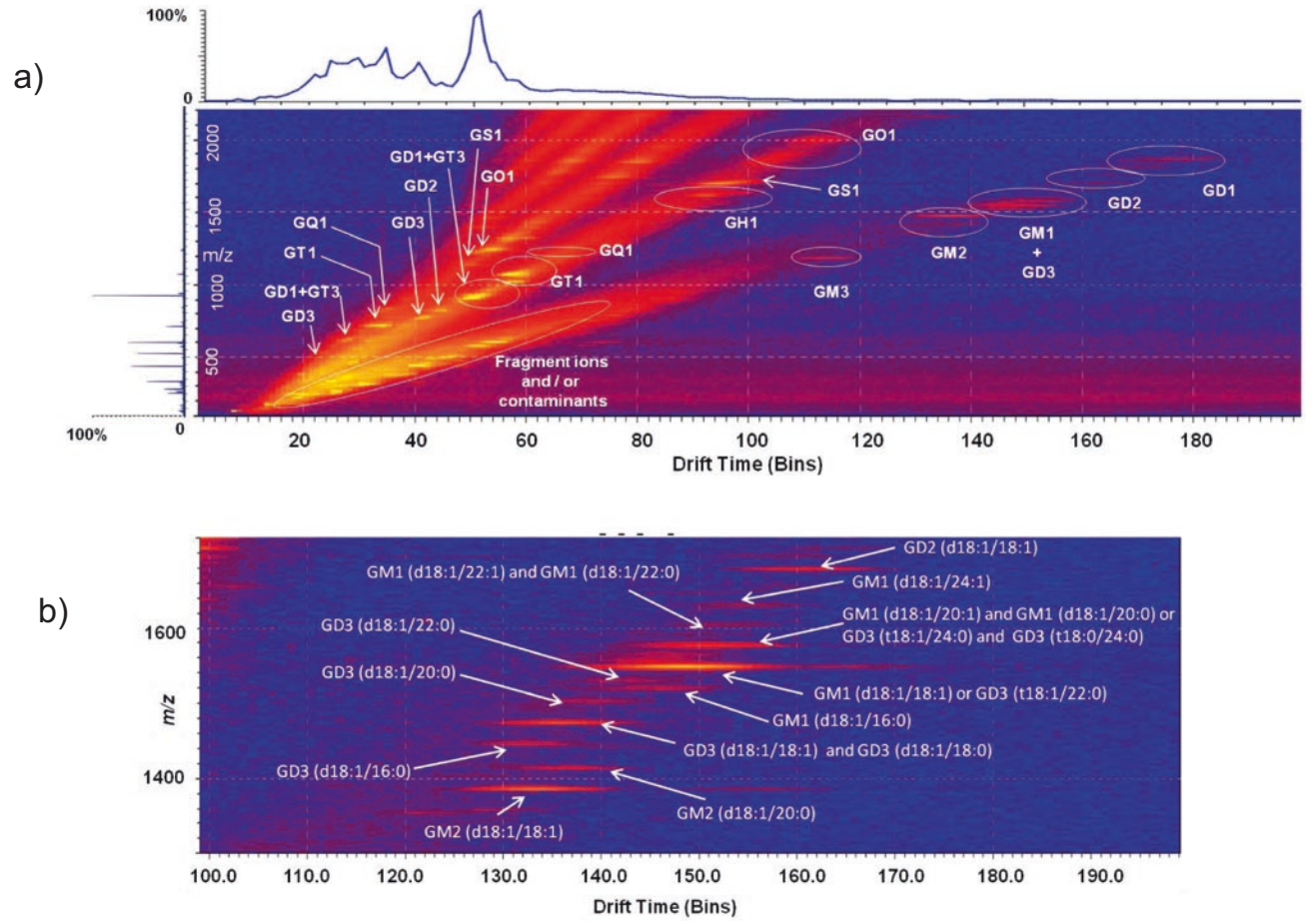

Fig. 42.7 IMS MS analysis of human fetal brain gangliosides. (**a**) driftscope display of the negative ions. The *m/z vs.* drift time plot reveals the separation of the gangliosides based on the carbohydrate chain length and the degree of sialylation; (**b**) expansion of driftscope display for *m/z* area between 1300 and 1720 clearly showing the separation based on the carbohydrate chain length of the singly charged gangliosides. Reprint with permission from [124]

layer of the dentate gyrus, which is to be correlated to the neurodegeneration that characterizes this particular form of dementia.

The complex role of GM1 ganglioside class in AD was additionally revealed this year [143] by the interesting results reported in a study that also involved MALDI MS imaging. The analyses discovered altered GM1 to GM2/GM3 ganglioside metabolism in the diffuse periphery of amyloid plaques, but not in the core region, which shows that GM1 is rather localized in the mature amyloid structure, interacts with the proteins at this level and is highly involved in AD pathology also via such interaction mechanisms.

The dysfunctions that arise in lipid metabolism are known to have a significant contribution in the development and progression of PD as well [144]. A number of studies and reports proved the major role played in PD by lipid dysregulation and by α-synuclein noncovalent interaction with acidic lipids such as phospholipids and sialylated glycolipids [113].

In this context important efforts were lately invested into development of high performance biophysical methods capable to provide a better insight into the expression, structure and interactions of glycolipids in PD and the modifications that occur in the glycolipid pattern with disease progression. Advanced mass spectrometry contributed an essential progress also in this field. The latest MS studies [97] conducted upon this disorder are focused on plasma lipidome of PD patients. The analyses, performed using triple quadrupole LC MS technique, revealed that this type of neurodegenerative disease is clearly associated with an increased level of GM3 gangliosides, which further indicates that GM3 is a biomarker class of gangliosides for PD, emphasizes the role played by GM3 in idiopathic PD and opens further directions for exploring the interactions between GM3 gangliosides and α-synuclein; the unambiguous elucidation of these interactions could provide a comprehensive insight into the pathophysiology of GM3 in PD.

Remarkable results substantiating the biomarker role of GM3 and the increased levels of these ganglioside species in plasma of PD patients were also reported in 2017 by the group of Zhang [145]. In LC MS derived quantitative

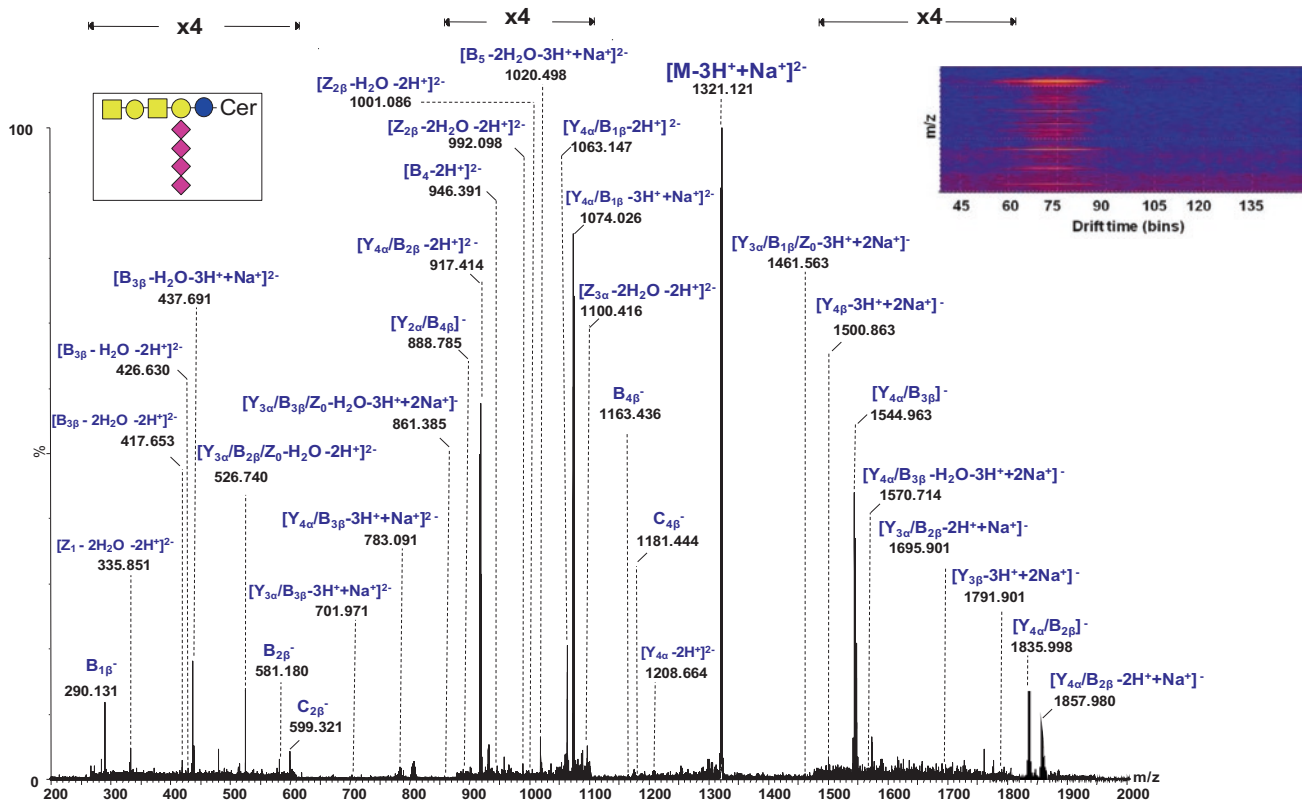

Fig. 42.8 ESI IMS CID MS/MS in the negative ion mode of the $[M + Na^+ - 3H^+]^{2-}$ at *m/z* 1321.121 corresponding to GalNAc−GQ1d (d18:1/18:0) species. Inset left: the structure of the precursor ion. Inset right: driftscope display of the IMS CID MS/MS product ions. Cone voltage 40 V. Capillary voltage 2 kV. Acquisition 300 scans. CID at variable collision energy within 10–45 eV. yellow filled square—GalNAc; yellow filled circle—Gal; blue filled circle—Glc; pink filled diamond—Neu5Ac. Reprint with permission from [124]

lipidomics studies was analyzed the profile of lipidomic plasma obtained from 170 PD patients vs. 120 controls. By LC MS using a triple quadrupole MS instrument, major differences patients *vs*. controls were observed in the case of GM3 concentration in plasma (1.293 ± 0.029 pmol/μl versus 1.488 ± 0.041 pmol/μl, respectively) after normalization with respect to the total lipid content.

PD was also approached using UPLC MS and MS/MS method, which was developed and validated for multiplex analysis of GlcCer isoforms (C18:0, C20:0, C22:0, C24:1, and C24:0) extracted from brain biopsies [146]. The brain tissue was sampled postmortem from the temporal cortex of 26 PD patients in different (IIa, III, and IV) stages of the disorder. The total lipid extract was separated by normal phase UPLC, which allowed for the discrimination of GlcCer and GalCer isobaric structures. Following the separation, the species were online detected by multiple reaction monitoring (MRM) MS and structurally analyzed by subsequent fragmentation in tandem MS. In the same study, GlcCer expression and concentration levels in control specimens and in patients with incidental Lewy Body dementia were also evaluated under identical measurement conditions. The results have shown an increase in GlcCer levels with PD severity. Therefore, GlcCer is to be further studied as a potential biomarker for early diagnosis, grading and prognosis of PD.

42.5 Concluding Remarks

We witness presently a strong trend in bioanalytical sciences toward the development of platforms able to provide a reliable molecular fingerprinting in high-throughput analyses.

In lipidomics such platforms are continuously optimized and refined for discovery of molecular markers or species associated to severe pathologies that are governed by mechanisms involving glycolipids. Such diseases are mainly related to the CNS where lipids and glycolipids are known to exhibit the most elevated expression, being, at the same time, highly susceptible to changes that occur at the CNS level, involved in their mechanisms of these changes and prone to undergo modifications of their composition, structure and distribution. Such alterations reflect CNS development, maturation and aging, are related to the particular functions of a certain brain area and, above all, are strongly associated to CNS pathologies. Brain cancers and neurodegenerative disorders, for which imagining methods may

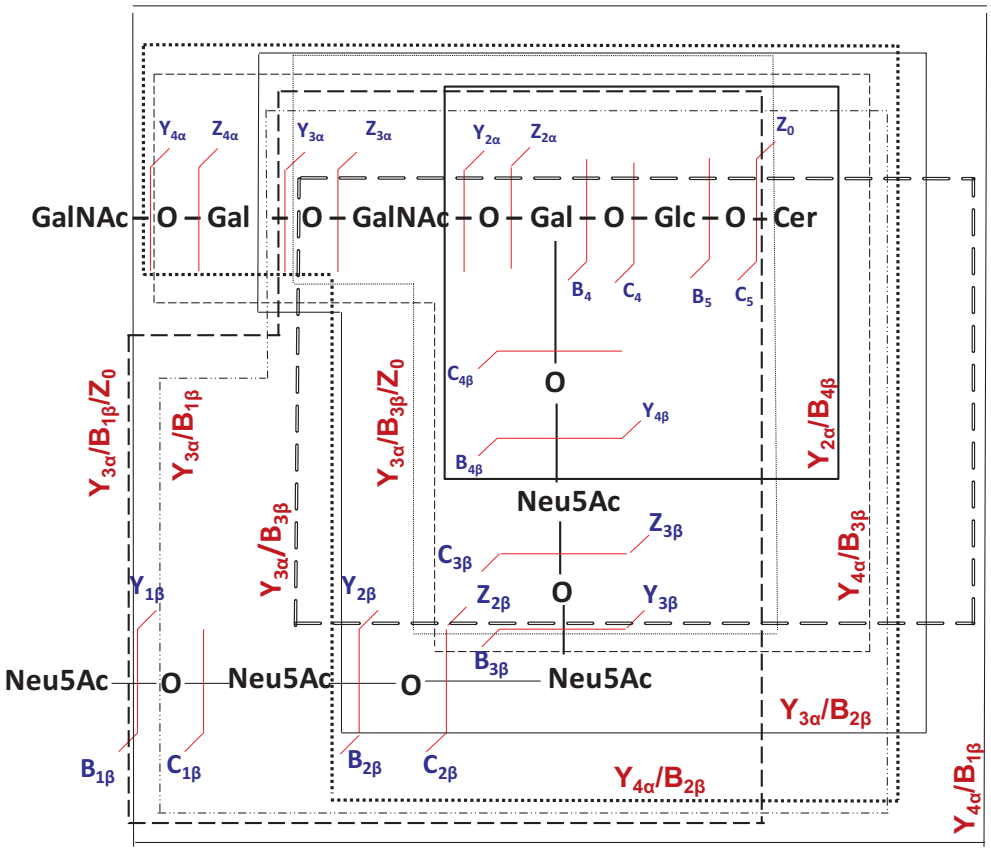

Fig. 42.9 Fragmentation scheme by IMS CID MS/MS of GalNAc−GQ1d species. Reprint with permission from [124]

either offer a limited and too general information (in the case of neurodegenerative disease) or a relatively late diagnostic, after the tumor was formed and started to progress (in the case of brain cancers), are among the pathologies targeted by the novel methods based on glycolipid fingerprinting and early detection of this type of disease biomarkers in plasma or cerebrospinal fluid.

As emphasized in this chapter, modern nanotechnology achievements in microfluidics for MS combined with robotized sample handling, fragmentation analysis by multistage MS and computer software for automatic spectral data interpretation contributed an essential progress to this field in the last few years. Several integrated microfluidic platforms for ESI were shown to offer ultrafast, sensitive, and accurate glycolipid biomarker discovery in complex, native mixtures extracted from healthy or pathological brain areas, often without the need of mixture separation prior to MS.

On the other hand, superior LC-MS and CID MS/MS methodologies were able to provide invaluable information of the role of different sialylated glycolipids in several neurodegenerative disorders, such as Parkinson's disease, Alzheimer's disease, and other forms of dementia.

However, ion mobility mass spectrometry, recently introduced in glycolipidomics of human brain in health and disease appears nowadays to be the most promising technique for glycolipid biomarker discovery in CNS and its related pathologies and for the extensive characterization of structural modifications in either the glycan core or lipid moiety that could be responsible or even trigger neurodegeneration. Important achievements of IMS MS and MS^n method, qualitative and quantitative data that will probably change the current perspective upon the role and functional interactions of glycolipids in the brain affected by neurodegeneration are expected to emerge in the near future.

Acknowledgements This project was supported by the Romanian National Authority for Scientific Research, UEFISCDI, through projects PN-III-P4-ID-PCE-2016-0073 and PN-III-P1-1.2-PCCDI-2017-0046 granted to A.D.Z. and PN-III-P1-1.1-PD-2016-0256 granted to M.S.

References

1. Lee, V. M.-Y., Giasson, B. I., & Trojanowski, J. Q. (2004). More than just two peas in a pod: Common amyloidogenic properties of tau and α-synuclein in neurodegenerative diseases. *Trends in Neurosciences, 27*, 129–134.
2. Giasson, B. I., Forman, M. S., Higuchi, M., Golbe, L. I., Graves, C. L., Kotzbauer, P. T., et al. (2003). Initiation and synergistic fibrillization of tau and alpha-synuclein. *Science, 300*, 636–640.

3. Grimm, M. O., Grimm, H. S., Pätzold, A. J., et al. (2005). Regulation of cholesterol and sphingomyelin metabolism by amyloid-β and presenilin. *Nature Cell Biology, 7*(11), 1118–1124.
4. Kanekiyo, T., Xu, H., & Bu, G. (2014). ApoE and Aβ in Alzheimer's disease: Accidental encounters or partners? *Neuron, 81*(4), 740–754.
5. Huynh, T. P., Davis, A. A., Ulrich, J. D., & Holtzman, D. M. (2017). Apolipoprotein E and Alzheimer disease: The influence of apoE on amyloid-β and other amyloidogenic proteins. *Journal of Lipid Research, 58*, 824–836.
6. Luan, K., Rosales, J. L., & Lee, K. Y. (2013). Crosstalks between neurofibrillary tangles and amyloid plaque formation. *Ageing Research Reviews, 12*(1), 174–181.
7. National institute for Health and Care Excellence. Dementia—Assessment, management and support for people living with dementia and their carers/NICE guideline NG97. (2018).
8. Douglas, S., James, I., & Ballard, C. (2004). Non-pharmacological interventions in dementia. *Advances in Psychiatric Treatment, 10*(3), 171–177.
9. Toledo, J. B., Zetterberg, H., Van Harten, A. C., et al. (2015). Alzheimer's disease cerebrospinal fluid biomarker in cognitively normal subjects. *Brain, 138*(9), 2701–2715.
10. de Wilde, A., van der Flier, W. M., Pelkmans, W., et al. (2018). Association of amyloid positron emission tomography with changes in diagnosis and patient treatment in an unselected memory clinic cohort: The ABIDE project. *JAMA Neurology, 75*(9), 1062–1070.
11. Saint-Aubert, L., Lemoine, L., Chiotis, K., et al. (2017). Tau PET imaging: Present and future directions. *Molecular Neurodegeneration, 12*, 19.
12. Sharma, N., & Singh, A. N. (2016). Exploring biomarkers for Alzheimer's disease. *Advances in Psychiatric Treatment, 10*(7), KE01–KE06.
13. Jack, C. R., Bennett, D. A., Blennow, K., et al. (2018). NIA-AA research framework: Toward a biological definition of Alzheimer's disease. *Alzheimers Dement, 14*(4), 535–562.
14. Neumann, M., Rademakers, R., Roeber, S., et al. (2009). A new subtype of frontotemporal lobar degeneration with FUS pathology. *Brain, 132*(11), 2922–2931.
15. Hughes, T. A., Ross, H. F., Musa, S., et al. (2000). A 10-year study of the incidence of and factors predicting dementia in Parkinson's disease. *Neurology, 54*(8), 1596–1603.
16. Galpern, W. R., & Lang, A. E. (2006). Interface between tauopathies and synucleinopathies: A tale of two proteins. *Annals of Neurology, 59*(3), 449–458.
17. Senard, J. M., Rai, S., & Lapeyre-Mestre, M. (1997). Prevalence of orthostatic hypotension in Parkinson's disease. *Journal of Neurology, Neurosurgery, and Psychiatry, 63*(5), 584–589.
18. Kotagal, V., Albin, R. L., & Müller, M. L. (2012). Symptoms of rapid eye movement sleep behavior disorder are associated with cholinergic denervation in Parkinson disease. *Annals of Neurology, 71*(4), 560–568.
19. Poewe, W. (2008). Non-motor symptoms in Parkinson's disease. *The European Journal of Neurology, 15*, 14–20.
20. Brandenburg, K., Holst, O. (2015). Glycolipids: Distribution and biological function. In eLS. Chichester: John Wiley & Sons.
21. Cooper, G. M. (2000). Cell–cell Interactions. In *The cell: A molecular approach* (2nd ed). Sunderland, MA: Sinauer Associates.
22. Malhotra, R. (2012). Membrane glycolipids: Functional heterogeneity: A review. *Biochemistry and Analytical Biochemistry, 1*, 108.
23. Shamim, A., Mahmood, T., Ahsan, F., et al. (2018). Lipids: An insight into the neurodegenerative disorders. *Clinical Nutrition Experimental, 20*, 1e19.
24. Williams, G. J., & Thorson, J. S. (2009). Natural product glycosyltransferases: Properties and applications. *Advances in Enzymology and Related Areas of Molecular Biology, 76*, 55–119.
25. Hakomori, S. (1995). Functional role of glycosphingolipids in cell recognition and signaling. *Journal of Biochemistry, 118*, 1091–1103.
26. Nelson, D. L., & Cox, M. M. (2000). *Lehninger principles of biochemistry* (6th ed.). New York: Freeman WH and Company.
27. Plomp, J. J., & Willison, H. J. (2009). Pathophysiological actions of neuropathyrelated anti-ganglioside antibodies at the neuromuscular junction. *Journal of Physiology, 587*, 3979–3999.
28. Koutsouraki, E. F. (2009). Gangliosides and neurodegeneration. *Encephalos, 46*, 44–48.
29. Ledeen, R. W. (1985). Gangliosides of the neuron. *Trends in Neurosciences, 8*, 169–174.
30. Ledeen, R. W., & Wu, G. (2006). GM1-ganglioside: another nuclear lipid that modulates nuclear calcium. GM1 potentiates the nuclear sodium-calcium exchanger. *Canadian Journal of Physiology and Pharmacology, 84*, 393–402.
31. Susuki, K., Baba, H., Tohyama, K., et al. (2007). Gangliosides contribute to stability of paranodal junctions and ion channel clusters in myelinated nerve fibers. *Glia, 55*, 746–757.
32. Hirabayashi, Y. (2012). A world of sphingolipids and glycolipids in the brain—Novel functions of simple lipids modified with glucose. *Proceedings of the Japan Academy. Series B, Physical and Biological Sciences, 88*, 129–143.
33. Sarbu, M., Cozma, C., & Zamfir, A. D. (2017). Structure-to-function relationship of carbohydrates in the mechanism of lysosomal storage disorders (LSDs). *Current Organic Chemistry, 21*, 2719.
34. Naylor, S. (2005). Overview of biomarkers in disease, drug discovery and development. Drug Discovery World Spring.
35. Fantini, J. (2003). How sphingolipids bind and shape proteins: Molecular basis of lipid-protein interactions in lipid shells, rafts and related biomembrane domains. *Cellular and Molecular Life Sciences, 60*, 1027–1032.
36. Choo-Smith, L. P., Garzon-Rodriguez, W., Glabe, C. G., & Surewicz, W. K. (1997). Acceleration of amyloid fibril formation by specific binding of Aβ-(1–40) peptide to ganglioside-containing membrane vesicles. *The Journal of Biological Chemistry, 272*, 22987–22990.
37. Matsuzaki, K., & Horikiri, C. (1999). Interactions of amyloid *β*-peptide (1–40) with ganglioside-containing membranes. *Biochemistry, 38*, 4137–4142.
38. McLaurin, J., Franklin, T., Fraser, P. E., & Chakrabartty, A. (1998). Structural transitions associated with the interaction of Alzheimer *β*-amyloid peptides with gangliosides. *The Journal of Biological Chemistry, 273*, 4506–4515.
39. Yanagisawa, K., Odaka, A., Suzuki, N., & Ihara, Y. (1995). GM1 ganglioside-bound amyloid beta-protein (A beta): A possible form of preamyloid in Alzheimer's disease. *Nature Medicine, 1*, 1062–1066.
40. Choo-Smith, L. P., & Surewicz, W. K. (1997). The interaction between Alzheimer amyloid beta(1–40) peptide and ganglioside GM1-containing membranes. *FEBS Letters, 402*, 95–98.
41. Ariga, T., Kobayashi, K., Hasegawa, A., et al. (2001). Characterization of high-affinity binding between gangliosides and amyloid beta-protein. *Archives of Biochemistry and Biophysics, 388*, 225–230.
42. Utsumi, M., Yamaguchi, Y., Sasakawa, H., et al. (2009). Up and- down topological mode of amyloid beta-peptide lying on hydrophilic/hydrophobic interface of ganglioside clusters. *Glycoconjugate Journal, 26*, 999–1006.
43. Hughes, R. A., & Cornblath, D. R. (2005). Guillain-Barre syndrome. *The Lancet, 366*, 1653–1666.
44. Yanagisawa, K. (2005). GM1 ganglioside and the seeding of amyloid in Alzheimer's disease: Endogenous seed for Alzheimer amyloid. *The Neuroscientist, 11*, 250–260.
45. Yanagisawa, K. (2007). Role of gangliosides in Alzheimer's disease. *Biochimica et Biophysica Acta, 1768*, 1943–1951.

46. Yanagisawa, K. (2015). GM1 ganglioside and Alzheimer's disease. *Glycoconjugate Journal, 32*, 87–91.
47. Yamamoto, N., Fukata, Y., Fukata, M., & Yanagisawa, K. (2007). GM1-ganglioside-induced Abeta assembly on synaptic membranes of cultured neurons. *Biochimica et Biophysica Acta, 1768*, 1128–1137.
48. Ariga, T., McDonald, M. P., & Yu, R. K. (2008). Role of ganglioside metabolism in the pathogenesis of Alzheimer's disease—A review. *Journal of Lipid Research, 49*, 1157–1175.
49. Kalanj-Bognar, S. (2006). Ganglioside catabolism is altered in fibroblasts and leukocytes from Alzheimer's disease patients. *Neurobiology of Aging, 27*, 1354–1356.
50. Svennerholm, L., & Gottfries, C. G. (1994). Membrane lipids, selectively diminished in Alzheimer brains, suggest synapse loss as a primary event in early-onset form (type I) and demyelination in late-onset form (type II). *Journal of Neurochemistry, 62*, 1039–1047.
51. Kracun, I., Rosner, H., Drnovsek, V., et al. (1991). Human brain gangliosides in development, aging and disease. *The International Journal of Developmental Biology, 35*, 289–295.
52. Kracun, I., Kalanj, S., Talan-Hranilovic, J., & Cosovic, C. (1992). Cortical distribution of gangliosides in Alzheimer's disease. *Neurochemistry International, 20*, 433–438.
53. Gylys, K. H., Fein, J. A., Yang, F., et al. (2007). Increased cholesterol in Abeta-positive nerve terminals from Alzheimer's disease cortex. *Neurobiology of Aging, 28*, 8–17.
54. Blennow, K., Davidsson, P., Wallin, A., et al. (1991). Gangliosides in cerebrospinal fluid in 'probable Alzheimer's disease. *Archives of Neurology, 48*, 1032–1035.
55. Liu, L., Zhang, K., Tan, L., Chen, Y. H., & Cao, Y. P. (2015). Alterations in cholesterol and ganglioside GM1 content of lipid rafts in platelets from patients with Alzheimer disease. *Alzheimer Disease and Associated Disorders, 29*, 63–69.
56. Molander-Melin, M., Blennow, K., Bogdanovic, N., et al. (2005). Structural membrane alterations in Alzheimer brains found to be associated with regional disease development; increased density of gangliosides GM1 and GM2 and loss of cholesterol in detergent resistant membrane domains. *Journal of Neurochemistry, 92*, 171–182.
57. Pernber, Z., Blennow, K., Bogdanovic, N., et al. (2012). Altered distribution of the gangliosides GM1 and GM2 in Alzheimer's disease. *Dementia and Geriatric Cognitive Disorders, 33*, 174–188.
58. Brooksbank, B. W. L., & McGovern, J. (1989). Gangliosides in the brain in adult Down's syndrome and Alzheimer's disease. *Molecular and Chemical Neuropathology, 11*, 143–156.
59. Crino, P. B., Ullman, M. D., Vogt, B. A., et al. (1989). Brain gangliosides in dementia of the Alzheimer type. *Archives of Neurology, 46*, 398–401.
60. Hirano-Sakamaki, W., Sugiyama, E., Hayasaka, T., et al. (2015). Alzheimer's disease is associated with disordered localization of ganglioside GM1 molecular species in the human dentate gyrus. *FEBS Letters, 589*, 3611–3616.
61. Yu, R. K., Usuki, S., & Ariga, T. (2006). Ganglioside molecular mimicry and its pathological roles in Guillain-Barré syndrome and related diseases. *Infection and Immunity, 74*, 6517–6527.
62. Yuki, N., & Ariga, T. (1997). Antibodies to fucogangliosides in neurological diseases. *Journal of the Neurological Sciences, 150*, 81–84.
63. Chapman, J., Sela, B. A., Wertman, E., & Michaelson, D. M. (1988). Antibodies to ganglioside GM1 in patients with Alzheimer's disease. *Neuroscience Letters, 86*, 235–240.
64. Miura, Y., Miyaji, K., Chai, Y. L., et al. (2014). Autoantibodies to GM1 and GQ1bα are not biological markers of Alzheimer's disease. *Journal of Alzheimer's Disease, 42*, 1165–1169.
65. Ando, S., Tanaka, Y., Waki, H., et al. (1998). Gangliosides and sialylcholesterol as modulators of synaptic functions. *Annals of the New York Academy of Sciences, 845*, 232–239.
66. Foley, P., Bradford, H. F., Docherty, M., et al. (1988). Evidence for the presence of antibodies to cholinergic neurons in the serum of patients with Alzheimer's disease. *Journal of Neurology, 235*, 466–471.
67. Chapman, J., Bachar, O., Korczyn, A. D., et al. (1988). Antibodies to cholinergic neurons in Alzheimer's disease. *Journal of Neurochemistry, 51*, 479–485.
68. Ariga, T., Yanagisawa, M., Wakade, C., et al. (2010). Ganglioside metabolism in a transgenic mouse model of Alzheimer's disease: Expression of Chol-1α antigens in the brain. *ASN Neuro, 2*, 233–241.
69. Hirabayashi, Y., Nakao, T., Irie, F., et al. (1992). Structural characterization of a novel cholinergic neuron-specific ganglioside in bovine brain. *The Journal of Biological Chemistry, 267*, 12973–12978.
70. Svennerholm, L., Bostrom, K., Jungbjer, B., & Olsson, L. (1994). Membrane lipids of adult human brain: Lipid composition of frontal and temporal lobe in subjects of age 20 to 100 years. *Journal of Neurochemistry, 63*, 1802–1811.
71. Oikawa, N., Yamaguchi, H., Ogino, K., et al. (2009). Gangliosides determine the amyloid pathology of Alzheimer's disease. *Neuroreport, 20*, 1043–1046.
72. Wu, G., Lu, Z. H., Kulkarni, N., & Ledeen, R. W. (2012). Deficiency of ganglioside GM1 correlates with Parkinson's disease in mice and humans. *Journal of Neuroscience Research, 90*, 1997–2008.
73. Hong, S., Ostaszewski, B. L., Yang, T., et al. (2014). Soluble Ab oligomers are rapidly sequestered from brain ISF in vivo and bind GM1 ganglioside on cellular membranes. *Neuron, 82*, 308–319.
74. Forsayeth, J., & Hadaczek, P. (2018). Ganglioside metabolism and Parkinson's disease. *Frontiers in Neuroscience, 12*, 45.
75. Martinez, Z., Zhu, M., Han, S., & Fink, A. L. (2007). GM1 specifically interacts with a-synuclein and inhibits fibrillation. *Biochemistry, 46*, 1868–1877.
76. Hatzifilippou, E., Arnaoutoglou, M., Koutsouraki, E., et al. (2015). High Levels of anti-ganglioside antibodies in patients with Parkinson's disease associated with cognitive decline. *Int J Neurorehabilitation, 2*, 2.
77. Harlalka, G. V., Lehman, A., Chioza, B., et al. (2013). Mutations in B4GALNT1 (GM2 synthase) underlie a new disorder of ganglioside biosynthesis. *Brain, 136*.(Pt 12, 3618–3624.
78. Sheikh, K. A., Sun, J., Liu, Y., et al. (1999). Mice lacking complex gangliosides develop Wallerian degeneration and myelination defects. *Proceedings of the National Academy of Sciences of the United States of America, 96*, 7532–7537.
79. Fantini, J., & Yahi, N. (2011). Molecular basis for the glycosphingolipid-binding specificity of a-synuclein: Key role of tyrosine 39 in membrane insertion. *Journal of Molecular Biology, 408*, 654–669.
80. Hadaczek, P., Wu, G., Sharma, N., et al. (2015). GDNF signaling implemented by GM1 ganglioside; failure in Parkinson's disease and GM1-deficient murine model. *Experimental Neurology, 263*, 177–189.
81. Seyfried, T. N., Choi, H., & Chevalier, A. (2018). Sex-related abnormalities in substantia nigra lipids in Parkinson's disease. *ASN Neuro, 10*, 1759091418781889.
82. Yahi, N., & Fantini, J. (2014). Deciphering the glycolipid code of Alzheimer's and Parkinson's amyloid proteins allowed the creation of a universal ganglioside binding peptide. *PLoS One, 9*, e104751.
83. Bisaglia, M., Schievano, E., Caporale, A., et al. (2006). The 11-mer repeats of human a-synuclein in vesicle interactions and lipid

composition discrimination: A cooperative role. *Biopolymers, 84*, 310–316.
84. Dettmer, U., Newman, A. J., Soldner, F., et al. (2015). Parkinson-causing a-synuclein missense mutations shift native tetramers to monomers as a mechanism for disease initiation. *Nature Communications, 6*, 7314.
85. Beavan, M. S., & Schapira, A. H. (2013). Glucocerebrosidase mutations and the pathogenesis of Parkinson disease. *Annals of Medicine, 45*, 511–521.
86. Mazzulli, J. R., Xu, Y. H., Sun, Y., et al. (2011). Gaucher disease glucocerebrosidase and α-synuclein form a bidirectional pathogenic loop in synucleinopathies. *Cell, 146*, 37–52.
87. Magalhaes, J., Gegg, M. E., Migdalska-Richards, A., et al. (2016). Autophagic lysosome reformation dysfunction in glucocerebrosidase deficient cells: Relevance to Parkinson disease. *Human Molecular Genetics, 25*, 3432–3445.
88. Grabowski, G. A. (2008). Phenotype, diagnosis, and treatment of Gaucher's disease. *Lancet, 372*, 1263–1271.
89. Beutler, E., & Grabowski, G. A. (2001). *The metabolic and molecular basis of inherited disease* (pp. 3635–3668). New York: McGraw-Hill.
90. Murphy, K. E., Gysbers, A. M., Abbott, S. K., et al. (2014). Reduced glucocerebrosidase is associated with increased alpha-synuclein in sporadic Parkinson's disease. *Brain, 137*, 834–848.
91. Chiasserini, D., Paciotti, S., Eusebi, P., et al. (2015). Selective loss of glucocerebrosidase activity in sporadic Parkinson's disease and dementia with Lewy bodies. *Molecular Neurodegeneration, 10*, 15.
92. Gegg, M. E., Burke, D., Heales, S. J., et al. (2012). Glucocerebrosidase deficiency in substantia nigra of parkinson disease brains. *Annals of Neurology, 72*, 455–463.
93. Ghauharali-van der Vlugt, K., Langeveld, M., Poppema, A., et al. (2008). Prominent increase in plasma ganglioside GM3 is associated with clinical manifestations of type I Gaucher disease. *Clinica Chimica Acta, 389*, 109–113.
94. Meikle, P. J., Whitfield, P. D., Rozaklis, T., et al. (2008). Plasma lipids are altered in Gaucher disease: Biochemical markers to evaluate therapeutic intervention. *Blood Cells, Molecules & Diseases, 40*, 420–427.
95. Clark, L. N., Chan, R., Cheng, R., et al. (2015). Gene-wise association of variants in four lysosomal storage disorder genes in neuropathologically confirmed Lewy body disease. *PLoS One, 10*, e0125204.
96. Gegg, M. E., Sweet, L., Wang, B. H., et al. (2015). No evidence for substrate accumulation in Parkinson brains with GBA mutations. *Movement Disorders, 30*, 1085–1089.
97. Chan, R. B., Perotte, A. J., Zhou, B., et al. (2017). Elevated GM3 plasma concentration in idiopathic Parkinson's disease: A lipidomic analysis. *PLoS One, 12*, e0172348.
98. Bellettato, C. M., & Scarpa, M. (2010). Pathophysiology of neuropathic lysosomal storage disorders. *Journal of Inherited Metabolic Disease, 33*, 347–362.
99. Shachar, T., Lo Bianco, C., Recchia, A., et al. (2011). Lysosomal storage disorders and Parkinson's disease: Gaucher disease and beyond. *Movement Disorders, 26*, 1593–1604.
100. Kodama, T., Togawa, T., Tsukimura, T., et al. (2011). Lyso-GM2 ganglioside: A possible biomarker of Tay-Sachs disease and Sandhoff disease. *PLoS One, 6*, e29074.
101. Sack Jr., G. H. (1980). Clinical diversity in Gaucher's disease. *The Johns Hopkins Medical Journal, 146*, 166–170.
102. Sidransky, E., Nalls, M. A., Aasly, J. O., et al. (2009). Multicenter analysis of glucocerebrosidase mutations in Parkinson's disease. *The New England Journal of Medicine, 361*, 1651–1661.
103. Sidransky, E. (2005). Gaucher disease and parkinsonism. *Molecular Genetics and Metabolism, 84*, 302–304.
104. Tayebi, N., Walker, J., Stubblefield, B., et al. (2003). Gaucher disease with parkinsonian manifestations: Does glucocerebrosidase deficiency contribute to a vulnerability to parkinsonism? *Molecular Genetics and Metabolism, 79*, 104–109.
105. Goker-Alpan, O., Schiffmann, R., LaMarca, M. E., et al. (2004). Parkinsonism among Gaucher disease carriers. *Journal of Medical Genetics, 41*, 937–940.
106. Alcalay, R. N., Dinur, T., Quinn, T., et al. (2014). Comparison of Parkinson risk in Ashkenazi Jewish patients with Gaucher disease and GBA heterozygotes. *JAMA Neurology, 71*, 752–757.
107. Dekker, N., van Dussen, L., Hollak, C. E., et al. (2011). Elevated plasma glucosylsphingosine in Gaucher disease: Relation to phenotype, storage cell markers, and therapeutic response. *Blood, 118*, e118–e127.
108. Muller, M. V. G., Petri, A., Vianna, L. P., et al. (2010). Quantification of glucosylceramide in plasma of Gaucher disease patients. *Brazilian Journal of Pharmaceutical Sciences, 46*, 643–649.
109. Gornati, R., Bembi, B., Tong, X., et al. (1998). Total glycolipid and glucosylceramide content in serum and urine of patients with Gaucher's Disease type 3 before and after enzyme replacement therapy. *Clinica Chimica Acta, 271*, 151–161.
110. Zamfir, A. D. (2014). Neurological analyses: Focus on gangliosides and mass spectrometry. *Advances in Experimental Medicine and Biology, 806*, 153–204.
111. Sisu, E., Flangea, C., Serb, A., et al. (2011). High-performance separation techniques hyphenated to mass spectrometry for ganglioside analysis. *Electrophoresis, 32*, 1591–1609.
112. Siew, J. J., & Chern, Y. (2018 May 14). Microglial lectins in health and neurological diseases. *Frontiers in Molecular Neuroscience, 11*, 158.
113. Suzuki, M., Sango, K., Wada, K., & Nagai, Y. (2018). Pathological role of lipid interaction with α-synuclein in Parkinson's disease. *Neurochemistry International, 119*, 97–106.
114. Li, T. A., & Schnaar, R. L. (2018). Congenital disorders of ganglioside biosynthesis. *Progress in Molecular Biology and Translational Science, 156*, 63–82.
115. Robu, A., Schiopu, C., Capitan, F., & Zamfir, A. D. (2016). Mass spectrometry of gangliosides in extracranial tumors: Application to adrenal neuroblastoma. *Analytical Biochemistry, 509*, 1–11.
116. Sarbu, M., Dehelean, L., Munteanu, C. V., et al. (2017). Assessment of ganglioside age-related and topographic specificity in human brain by Orbitrap mass spectrometry. *Analytical Biochemistry, 521*, 40–54.
117. Capitan, F., Robu, A., Popescu, L., et al. (2015). B subunit monomers of Cholerae toxin bind G1 ganglioside class as revealed by chip-nanoelectrospray multistage mass spectrometry. *Journal of Carbohydrate Chemistry, 34*, 388–408.
118. Cozma, I., Sarbu, M., Ilie, C., & Zamfir, A. D. (2017). Structural analysis by electrospray ionization mass spectrometry of GT1 ganglioside fraction isolated from fetal brain. *Journal of Carbohydrate Chemistry, 36*, 247–264.
119. Zhang, Y., Wang, J., Liu, J., et al. (2016). Combination of ESI and MALDI mass spectrometry for qualitative, semi-quantitative and in situ analysis of gangliosides in brain. *Scientific Reports, 6*, 25289.
120. Sarbu, M., & Zamfir, A. D. (2018). Modern separation techniques coupled to high performance mass spectrometry for glycolipid analysis. *Electrophoresis, 39*, 1155–1170.
121. Zamfir, A. D., Flangea, C., Altmann, F., & Rizzi, A. M. (2011). Glycosylation analysis of proteins, proteoglycans and glycolipids by CE-MS. *Advances in Chromatography, 49*, 135–186.
122. Almeida, R., Mosoarca, C., Chirita, M., et al. (2008). Coupling of fully automated chip-based electrospray ionization to high capacity ion trap mass spectrometer for ganglioside analysis. *Analytical Biochemistry, 378*, 43–52.

123. Huang, Q., Liu, D., Xin, B., et al. (2016). Quantification of monosialogangliosides in human plasma through chemical derivatization for signal enhancement in LC-ESI-MS. *Analytica Chimica Acta, 929*, 31–38.
124. Sarbu, M., Robu, A., Ghiulai, R., et al. (2016). Electrospray ionization ion mobility mass spectrometry of human brain gangliosides. *Analytical Chemistry, 88*, 5166–5178.
125. Fuller, D. R., Conant, C. R., El-Baba, T. J., et al. (2018). Conformationally regulated peptide bond cleavage in bradykinin. *Journal of the American Chemical Society, 140*, 9357–9360.
126. El-Baba, T. J., Fuller, D. R., Woodall, D. W., et al. (2018). Melting proteins confined in nanodroplets with 10.6 μm light provides clues about early steps of denaturation. *Chemical communications (Cambridge, England), 54*, 3270–3273.
127. Jacobs, A., Hoover, H., Smith, E., et al. (2018). The intrinsically disordered N-terminal arm of the brome mosaic virus coat protein specifically recognizes the RNA motif that directs the initiation of viral RNA replication. *Nucleic Acids Research, 46*, 324–335.
128. Musbat, L., Nihamkin, M., Toker, Y., et al. (2017). Measurements of the stabilities of isolated retinal chromophores. *Physical Review E, 95*, 012406.
129. Sarbu, M., Vukelić, Ž., Clemmer, D. E., & Zamfir, A. D. (2018). Ion mobility mass spectrometry provides novel insights into the expression and structure of gangliosides in the normal adult human hippocampus. *Analyst*. https://doi.org/10.1039/c8an01118d
130. Škrášková, K., Claude, E., Jones, E. A., et al. (2016). Enhanced capabilities for imaging gangliosides in murine brain with matrix-assisted laser desorption/ionization and desorption electrospray ionization mass spectrometry coupled to ion mobility separation. *Methods, 104*, 69–78.
131. Jackson, S. N., Colsch, B., & Egan, T. (2011). Gangliosides' analysis by MALDI-ion mobility MS. *Analyst, 136*, 463–466.
132. Kar, S., Slowikowski, S. P., Westaway, D., & Mount, H. T. (2004). Interactions between beta-amyloid and central cholinergic neurons: Implications for Alzheimer's disease. *Journal of Psychiatry and Neuroscience, 29*, 427–441.
133. Fuentealba, R. A., Farias, G., Scheu, J., et al. (2004). Signal transduction during amyloid-beta-peptide neurotoxicity: Role in Alzheimer disease. *Brain Research Reviews, 47*, 275–289.
134. Svennerholm, L., Brane, G., Karlsson, I., et al. (2002). Alzheimer disease—Effect of continuous intracerebroventricular treatment with GM1 ganglioside and a systematic activation programme. *Dementia and Geriatric Cognitive Disorders, 14*, 128–136.
135. Wakabayashi, M., Okada, T., Kozutsumi, Y., & Matsuzaki, K. (2005). GM1 ganglioside-mediated accumulation of amyloid beta-protein on cell membranes. *Biochemical and Biophysical Research Communications, 328*, 1019–1023.
136. Fukami, Y., Ariga, T., Yamada, M., & Yuki, N. (2017). Brain gangliosides in Alzheimer's disease: Increased expression of cholinergic neuron-specific gangliosides. *Current Alzheimer Research, 14*, 586–591.
137. Kalanj, S., Kracun, I., Rosner, H., & Cosović, C. (1991). Regional distribution of brain gangliosides in Alzheimer's disease. *Neurologia Croatica, 40*, 269–281.
138. Armirotti, A., Basit, A., Realini, N., et al. (2014). Sample preparation and orthogonal chromatography for broad polarity range plasma metabolomics: Application to human subjects with neurodegenerative dementia. *Analytical Biochemistry, 455*, 48–54.
139. Touboul, D., & Gaudin, M. (2014). Lipidomics of Alzheimer's disease. *Bioanalysis, 6*, 541–561.
140. Oikawa, N., Matsubara, T., Fukuda, R., et al. (2015). Imbalance in fatty-acid-chain length of gangliosides triggers Alzheimer amyloid deposition in the precuneus. *PLoS One, 10*, e0121356.
141. Jung, J. S., Shin, K. O., Lee, Y. M., et al. (2013). Anti-inflammatory mechanism of exogenous C2 ceramide in lipopolysaccharide-stimulated microglia. *Biochimica et Biophysica Acta, 1831*, 1016–1026.
142. Caughlin, S., Hepburn, J. D., Park, D. H., et al. (2015). Increased expression of simple ganglioside species GM2 and GM3 detected by MALDI imaging mass spectrometry in a combined rat model of Aβ toxicity and stroke. *PLoS One, 10*, e0130364.
143. Michno, W., Wehrli, P. M., Zetterberg, H., et al. (2018). GM1 locates to mature amyloid structures implicating a prominent role for glycolipid-protein interactions in Alzheimer pathology. *Biochimica et Biophysica Acta, Proteins and Proteomics*. https://doi.org/10.1016/j.bbapap.2018.09.010
144. Taguchi, Y. V., Liu, J., Ruan, J., et al. (2017). Glucosylsphingosine promotes α-synuclein pathology in mutant GBA-associated Parkinson's disease. *The Journal of Neuroscience, 37*, 9617–9631.
145. Zhang, J., Zhang, X., Wang, L., & Yang, C. (2017). High performance liquid chromatography-mass spectrometry (LC-MS) based quantitative lipidomics study of ganglioside-NANA-3 plasma to establish its association with Parkinson's disease patients. *Medical Science Monitor, 23*, 5345–5353.
146. Boutin, M., Sun, Y., Shacka, J. J., & Auray-Blais, C. (2016). Tandem mass spectrometry multiplex analysis of glucosylceramide and galactosylceramide isoforms in brain tissues at different stages of Parkinson disease. *Analytical Chemistry, 88*, 1856–1563.